THE ASTROPHYSICAL JOURNAL, 574:985–1003, 2002 August 1

SIMULATION OF A SPACE-BASED MICROLENSING SURVEY FOR TERRESTRIAL EXTRASOLAR PLANETS

DAVID P. BENNETT AND SUN HONG RHIE
Department of Physics, 225 Nieuwland Science Hall, University of Notre Dame, Notre Dame, IN 46556; bennett@nd.edu, srhie@nd.edu
Received 2000 November 28; accepted 2002 April 1

ABSTRACT

We show that a space-based gravitational microlensing survey for terrestrial extrasolar planets is feasible in the near future and could provide a nearly complete picture of the properties of planetary systems in our Galaxy. We present simulations of such a survey using a 1–2 m aperture space telescope with a ~ 2 deg^2 field of view to continuously monitor $\sim 10^8$ Galactic bulge main-sequence stars. The microlensing techniques allow the discovery of low-mass planets with high signal-to-noise ratio, and the space missions that we have studied are sensitive to planets with masses as low as that of Mars. By targeting main-sequence source stars, which can only be resolved from space, the space-based microlensing survey is able to detect enough light from the lens stars to determine the spectral type of one-third of the lens stars with detected planets, including virtually all of the F, G, and K stars, which comprise one-quarter of the event sample. This enables the determination of the planetary masses and separations in physical units as well as the abundance of planets as a function of stellar type and distance from the Galactic center. We show that a space-based microlensing planet search program has its highest sensitivity to planets at orbital separations of 0.7–10 AU, but it will also have significant sensitivity at larger separations and will be able to detect free-floating planets in significant numbers. This complements the planned terrestrial planet transit missions, which are sensitive to terrestrial planets at separations of ≤ 1 AU. Such a mission should also detect $\sim 50{,}000$ giant planets via transits, and it is, therefore, the only proposed planet detection method that is sensitive to planets at all orbital radii.

Subject headings: dark matter — gravitational lensing
On-line material: color figures

1. INTRODUCTION

The discovery of the first extrasolar planets a few years ago (Mayor & Queloz 1995; Marcy & Butler 1996; Butler & Marcy 1996) has spurred the growth of a new branch of observational astronomy, the study of extrasolar planets. The success of the precision radial velocity technique has been spectacular (Marcy, Cochran, & Mayor 2000; Perryman 2000; Marcy & Butler 2000) with the discovery of more than 70 extrasolar giant planets in the past seven years. This technique is sensitive enough to detect Jupiter mass planets in Jupiter-like orbits, and it is anticipated that such planets will be discovered in the next few years as the duration of the radial velocity monitoring programs approaches Jupiter's orbital period of 12 yr. The dramatic success of these radial velocity extrasolar planet search programs has encouraged the astronomical community to address the far more ambitious goal of searching for Earth-like extrasolar planets (Dressler et al. 1996[1]) because such planets seem best suited for life. The search for Earth-like extrasolar planets has now become a major NASA goal. It is likely that it will require the development of new extrasolar planet search techniques since it is thought that the intrinsic radial velocity noise of stars will limit this technique to planets with masses $\gtrsim$ a few times 10^{-4} of the host star's mass, which is 100 times greater than an Earth mass.

A number of extrasolar planet search methods have been proposed that should be able to detect planets in the Earth mass range (Perryman 2000). The *Space Interferometry Mission* (*SIM*; Danner & Unwin 1999) will be able to detect planets of a few Earth masses around nearby stars via their astrometric effects on the stars they orbit, but *SIM* requires some technical development before it will be ready to fly, and it is not required to have the capability to detect Earth mass planets. The most ambitious planet search missions being considered are the *Terrestrial Planet Finder* (*TPF*; Beichman 1998) and *Darwin* (Fridlund 2002) missions, which will have the ability to directly detect Earth-like planets around nearby stars. However, these missions require a considerable amount of technological development before they will be ready to fly. Also, the McKee-Taylor Decadal Survey Committee (McKee & Taylor 2000) qualified its endorsement of the *TPF* mission with the condition that the abundance of Earth-size planets be determined prior to the start of the *TPF* mission.

The gravitational microlensing and transit techniques are two methods that have sensitivity to terrestrial planets, but they are technically easier than *SIM* or *TPF*. These missions are sensitive to planets orbiting distant stars, so they are most useful for obtaining statistical information regarding the abundance of planetary systems. The transit technique is employed by the *COROT* mission (Schneider et al. 1998), which is slated for launch by CNES in 2004, the *Eddington* mission (Deeg et al. 2000), which has been selected as an ESA F2/F3 "reserve" mission, and the *Kepler* mission (Koch et al. 1998), which is under development for NASA's Discovery Program. However, these surveys share the property that the transit signal due to an Earth-like planet is a photometric variation of only $\sim 0.01\%$. This is only a few times above the anticipated photometric noise, so these missions generally require the observation of three or four transits in order to avoid false detections due to photometric noise. Even then, one false detection is expected over the

[1] Dressler et al. (1996) is also available at http://www.stsci.edu/stsci/org/hst-and-beyond-report.pdf.

course of the mission.[2] The requirement for three to four transits limits the sensitivity of the transit technique to planets with orbital periods of $\lesssim 1$ yr because of the limited mission duration and low transit probability for planets in longer period orbits. In contrast, the sensitivity of a space-based microlensing planet search program extends from about 0.7 AU to infinity, with significant sensitivity to free-floating planets. Thus, the combination of a transit survey like *Kepler* with a space-based microlensing planet search will determine the abundance of terrestrial and larger planets at all orbital radii.

Knowledge of the general properties of planetary systems is important even if we are primarily interested in habitable planets because the issue of planetary habitability is a complex and poorly defined one. The Earth's habitability is a consequence of a complex interplay of physical processes (Lunine 1999) that are not likely to be replicated in exactly the same way on other worlds. While the fundamental requirement is assumed to be stable liquid water over geologic time, many diverse factors come into play in establishing habitable ecosystems (Des Marais et al. 2001). More importantly, we do not know what the outcome of a different combination or timing of such processes would be in terms of habitability (Chyba, Whitmire, & Reynolds 2000). A nonexhaustive list of the potential requirements for habitability includes the presence of giant planets in 5–10 AU orbits (Lunine 2001), the presence of a large moon to stabilize the planetary spin axis (Ward 1982), and main-sequence stellar type of F, G, or K (Ward & Brownlee 2000; Kasting 1997). Also, the traditional notion that a narrow range of semimajor axes is consistent with the presence of liquid water (Kasting, Whitmire, & Reynolds 1993) is challenged by the evidence for liquid water on early Mars (Carr 1996). The length and incompleteness of this shopping list demand that survey missions be initiated soon to map out the geometries of extrasolar planetary systems prior to much more expensive missions whose intent is to spectroscopically examine extrasolar terrestrial planets. With its high sensitivity to low-mass planets at a wide range of separations, a space-based gravitational microlensing survey would be the ideal mission for a comprehensive survey of the properties of planetary systems.

1.1. *The Gravitational Microlensing Technique*

The gravitational microlensing technique (Mao & Paczyński 1991; Gould & Loeb 1992; Bennett & Rhie 2000b[3]) has the unique property that the strength of the planet's photometric microlensing signal is nearly independent of the planetary mass. Instead of a weaker signal, the microlensing signals of low-mass planets have a shorter duration and a lower detection probability than those of high-mass planets. (This argument breaks down for planetary masses below 0.1 $M_\oplus$ because such planets lens only a fraction of the main-sequence source star disks.) This means that a microlensing survey with frequent observations of a very large number of stars will be able to detect terrestrial planets at high signal-to-noise ratios (Tytler 1996;[4] Bennett & Rhie 1996, 2000a; Wambsganss 1997). The microlensing technique employs stars in the Galactic bulge that act as sources of light rays that are bent by the gravitational fields of stars in the foreground: on the near side of the Galactic bulge or in the disk. Planets that may orbit these "lens" stars can be detected when the light rays from one of the lensed images pass close to a planet orbiting the lens star. The gravitational field of the planet distorts this lensed image causing a significant variation of the gravitational microlensing light curve from the standard single-lens light curve. This planetary deviation is typically of order $\sim$10%, and it has a duration of a few hours to a day compared to the typical 1–2 month duration for lensing events due to stars.

The main challenge for a microlensing planet search project is that microlensing events are rare. Only about 3×10^{-6} of Galactic bulge stars are microlensed at any given time (Udalski et al. 1994; Alcock et al. 1997, 2000b), and only $\sim$2% of Earth mass planets orbiting these stars will be in the right position to be detected (Bennett & Rhie 1996). The sensitivity limit of the gravitational microlensing technique is set by the finite angular size of the source stars because a very low mass planet will only deflect the light rays from a fraction of the source star's disk. This can wash out the photometric signal of the planet. For main-sequence source stars in the Galactic bulge, the sensitivity limit is about 0.1 $M_\oplus$, but for giant source stars, it is greater than 1 $M_\oplus$. Thus, a gravitational microlensing search for terrestrial planets must use main-sequence source stars. However, the density of bright main-sequence stars in the central Galactic bulge is several stars per square arcsecond, so angular resolution of $\ll 1''$ is necessary to resolve these stars.

In order to accurately characterize the parameters of the planets discovered via microlensing (Gaudi & Gould 1997; Gaudi 1998), we must have photometry of $\sim$1% accuracy sampled several times per hour over a period of several days (i.e., a factor of a few longer than the planetary light-curve deviation). The microlensing event light curves must also be sampled continuously for periods of more than 24 hr, in order to unambiguously characterize the planetary signals in microlensing light curves. This allows both the full planetary deviation as well as the periods before and after it to be observed.

1.2. *Ground-based Microlensing Planet Searches*

The earliest discussions of detecting terrestrial planets via gravitational microlensing generally considered it to be a technique for ground-based observations (Tytler 1996; Bennett & Rhie 1996; Wambsganss 1997; Albow et al. 2001). However, these early estimates proved to be overly optimistic in a number of respects. Peale (1997) performed a simulation of what sort of planets could be detected by a global network of $\sim$2 m telescopes as suggested by Tytler (1996) and showed that a substantial number of possible planet detections would be missed because of poor weather and geographic limitations on the locations of ground-based telescopes, but his results are overoptimistic for several different reasons. For example, no account was taken of variations in atmospheric seeing or of the poorer average seeing from the non-Chilean observing sites. Sackett (1997) sought to avoid the problems of the poorer observing sites by proposing a search employing only a single, excellent observing site, Paranal, under the assumption that the planetary signals of terrestrial planets would be brief enough that

[2] See the *Kepler* website at http://www.kepler.arc.nasa.gov.

[3] Bennett & Rhie (2000b) as well as several other articles are also available at http://bustard.phys.nd.edu/GEST/publications.html.

[4] Tytler (1996) is also available at http://origins.jpl.nasa.gov/library/exnps/ExNPS.html.

some could be fully characterized by observations spanning $\sim$ 8 hr.

All of these papers considered the monitoring of Galactic bulge "turnoff" stars. Ground-based color-magnitude diagrams of the dense Galactic bulge fields observed by the microlensing surveys seemed to show that there were very large numbers of these stars. Turnoff stars are stars that have recently exhausted the hydrogen fuel in their cores and are just beginning the hydrogen shell burning phase. They are 1–2 mag brighter than the stars at the top of the main sequence but have similar colors. Their radii are small enough to allow the detection of Earth mass planets via microlensing. However, this is a relatively brief phase of stellar evolution, and so their apparent abundance in Galactic bulge seemed odd. In fact, this abundance was not confirmed with *Hubble Space Telescope* (*HST*) data (Holtzman et al. 1998). The apparent abundance of these turnoff stars is an artifact of the stellar crowding in these central Galactic bulge fields; the density of main-sequence stars is too high for them to be individually resolved, and several main-sequence stars blended together are typically identified as a single turnoff star. This is illustrated in Figure 1, which compares two ground-based images of microlensing event MACHO-96-BLG-5 to an *HST* image and a simulated image from a proposed space-based microlensing planet search telescope. Clearly, the density of bright main-sequence stars (like the one indicated) is too high for these stars to be individually resolved from the ground. This stellar blending phenomenon has been widely discussed in the gravitational microlensing literature (di Stefano & Esin 1995; Wozniak & Paczyński 1997; Han 1997), and there is now strong evidence that virtually all of the microlensing events involving apparent bulge turnoff source stars are, in fact, blended microlensing events with

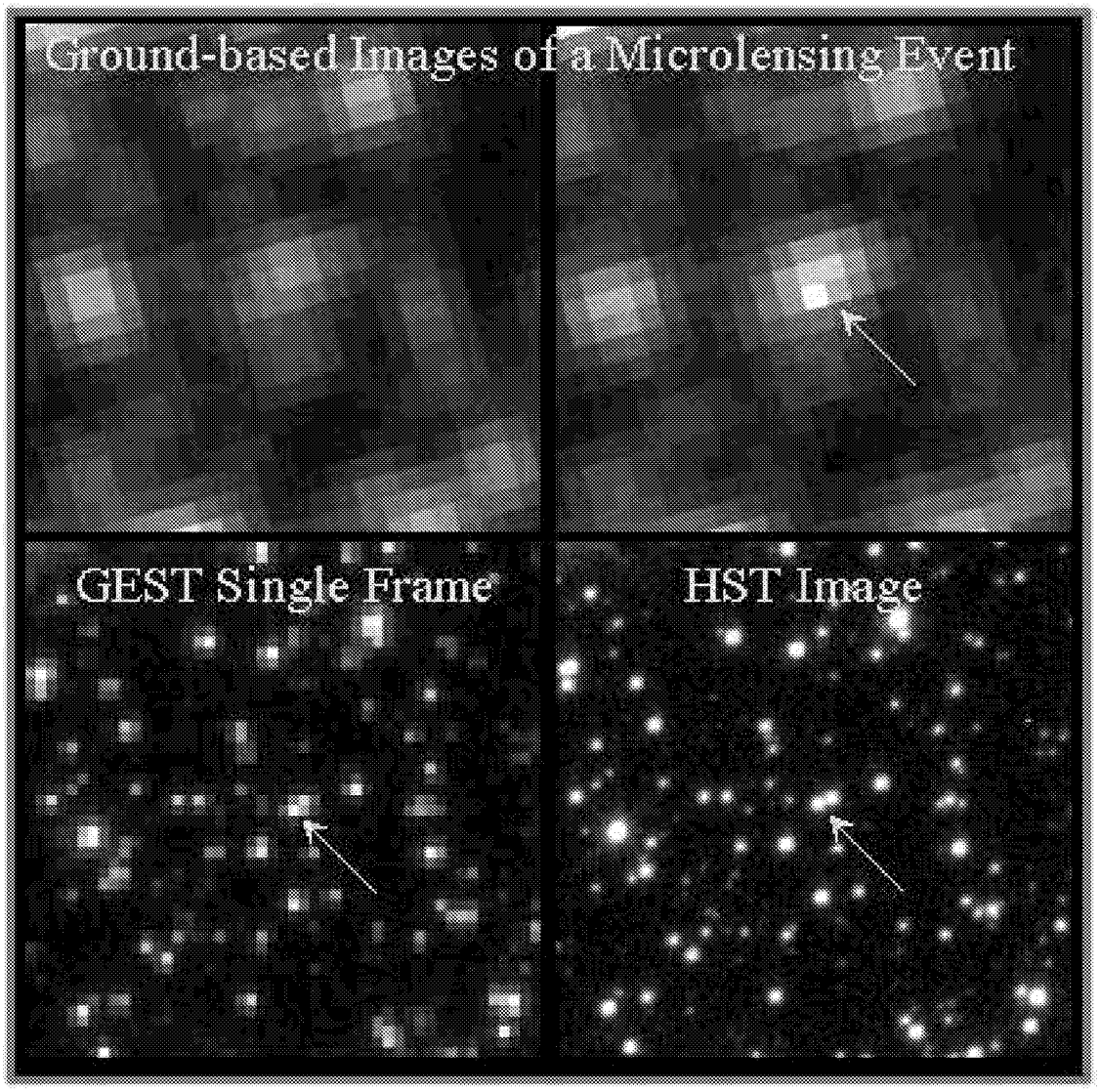

FIG. 1.—Difference between ground- and space-based data for microlensing of a bulge main-sequence star illustrated with images of microlensing event MACHO-96-BLG-5. The two top panels are 50 minute *R*-band exposures with the Cerro Tololo Inter-American Observatory 0.9 m telescope taken in 1″ seeing at different microlensing magnifications, and the two images on the bottom have been constructed from *HST* frames. The bottom left-hand image represents a 10 minute exposure with *GEST*'s angular resolution and pixel size, and the image on the right is an *HST* image. The lensing magnification factors are $A = 4$ and 10 for the ground-based images and 1.07 for the space-based image. The source star, a Galactic bulge G dwarf, is indicated by the arrows. [*See the electronic edition of the Journal for a color version of this figure.*]

main-sequence source stars (Alcock et al. 2000a, 2000b). This blending of source stars makes microlensing planet searches much more difficult because the planetary signal will be confined to the flux from only one of the blended stars, but all of the blended stars will contribute to the photometric noise.

One can hope to compensate for the increased photometric noise caused by blending by moving to relatively large wide field-of-view ground-based telescopes, such as the 4 m Visible and Infrared Survey Telescope for Astronomy or the ~8 m Large Synoptic Survey Telescope (LSST—recommended by the McKee-Taylor Committee [McKee & Taylor 2000]). A detailed study of such potential observing programs reveals that a survey from an excellent observing site such as Paranal is about 2 orders of magnitude less sensitive than a space-based microlensing planet search program (D. P. Bennett & S. H. Rhie 2002, in preparation). A critical problem for such a ground-based program is that the typical duration of a microlensing light-curve deviation due to an Earth mass planet is nearly 24 hr. This is about an order of magnitude longer than the Einstein radius crossing time, which was used as the characteristic planetary event duration in a previous study that advocated a microlensing planet survey from a single site (Sackett 1997). With a realistic distribution of event durations, however, we find that only a very small subset of Earth mass planetary microlensing signals can be detected and characterized. The detectable Earth mass planet events from such a survey also suffer from several undesirable selection effects. There is a much higher fraction of high-magnification events with planetary separations very close to the Einstein radius, and these events provide essentially no information on the abundance of planets as a function of orbital separation. Finally, few of the events that are detected with these ground-based surveys allow the detection of the lens star, so the planetary abundance as a function of spectral type also cannot be measured from the ground.

1.3. *Microlensing Planet Search Space Mission Requirements*

The primary intent of this paper is to investigate low-cost space missions that employ the gravitational microlensing technique to detect terrestrial planets orbiting other stars. The basic requirements for such a mission are that $\sim 10^8$ Galactic bulge main-sequence stars must be observed almost continuously at intervals of 20 minutes or less for periods of at least several months. Photometric accuracy of ~1% or better is needed, and this implies that the angular resolution of the images must be less than 0.″4 in order to resolve main-sequence stars in the crowded central Galactic bulge fields. The required frequent photometric measurement of such a large number of stars requires a relatively high data rate of $\gtrsim$ 10 Mbits s^{-1} depending on the data compression scheme that is used.

While the wide-field imaging capabilities required for such a mission substantially exceed the capabilities of existing space telescopes, it can be undertaken at a relatively modest cost, within the limits of NASA's MIDEX or Discovery Programs. There may also be an opportunity to combine a microlensing planet search mission with another major science program, such as a deep, wide-field, weak gravitational lensing survey or a high-redshift supernova search similar to the proposed *Supernova/Acceleration Probe* (*SNAP*).[5] It might also be possible to combine a microlensing planet search mission with an asteroseismology program such as the *Eddington* mission[6] if such a mission was designed with good in-focus optics.

Two proposals for microlensing planet search missions have been submitted to NASA in 2001. The *Galactic Exoplanet Survey Telescope* (*GEST*)[7] was submitted to NASA's MIDEX Program, and the *Survey for Terrestrial ExoPlanets* (*STEP*) was submitted to NASA's Extrasolar Planets: Advanced Concepts Program. We use the *GEST* MIDEX proposal as the baseline for our discussions of planet detection sensitivity, but we also investigate the variation of the planet detection sensitivity on the parameters of the mission.

The terrestrial planetary signals in gravitational microlensing light curves that these missions would study show significant variations on timescales ranging from 20–30 minutes to about a day. Therefore, it is important that a microlensing planet search telescope be in an orbit that allows continuous viewing of the Galactic bulge. The orbit proposed for *GEST* is a polar orbit with an altitude of ~1200 km oriented to keep the Galactic bulge in the continuous viewing zone, while the *STEP* mission would employ a nearly circular geosynchronous orbit inclined by 28.°7 (the latitude of Cape Canaveral) from the equator and by ~50° with respect to the ecliptic plane. Even higher Earth orbits, such as the 14 day "Prometheus" orbit proposed for *SNAP*, would also be acceptable, but an Earth-trailing orbit might make it difficult to achieve the required data rate.

The *GEST* and *STEP* designs call for 1.0 and 1.5 m aperture telescopes, respectively, each with a 2.2 deg^2 field of view and a three-mirror anastigmat design. The field of view is elliptical with an axis ratio of about 2 : 1, and the *GEST* proposal would use an array of 32 3072 × 6144 pixel Lincoln Labs high-resistivity CCDs for enhanced sensitivity in the near-IR. The *STEP* proposal would use a combination of these same Lincoln Labs CCDs and Rockwell HgCdTe IR detector arrays. These IR detectors would be similar to a design intended for the *HST*'s Wide Field Camera 3 with a long wavelength cutoff of ~1.7 μm to allow radiative cooling from a high Earth orbit. The quantum efficiency of these detectors is displayed in Figure 2 along with the reddened spectrum of a typical bulge source star. The standard CCD curve is typical of most broadband astronomical CCD detectors (such as those manufactured by Marconi, SITe, or Fairchild). Both the Lincoln Labs and Lawrence Berkley Laboratory (LBL) devices use high-resistivity silicon to enhance sensitivity in the near-IR, and the LBL devices have higher sensitivity near $\lambda = 1.0$ μm because they are more opaque at this wavelength because of their 300 μm thickness versus 50 μm for the Lincoln devices.

The overall sensitivity of the detectors is given by the integral of the product of the source spectrum, the quantum efficiency (QE) curve, and an additional function describing the throughput of the rest of the optical system. If we assume that the optical system has no other significant wavelength dependence besides the detectors, then we find

[5] See the *SNAP* Web site at http://snap.lbl.gov for information regarding the proposed *SNAP* mission.

[6] See the *Eddington* Web site at http://astro.esa.int/SA-general/Projects/Eddington for information on ESA's *Eddington* mission.

[7] More information on the *Galactic Exoplanet Survey Telescope* is available at http://bustard.phys.nd.edu/GEST.

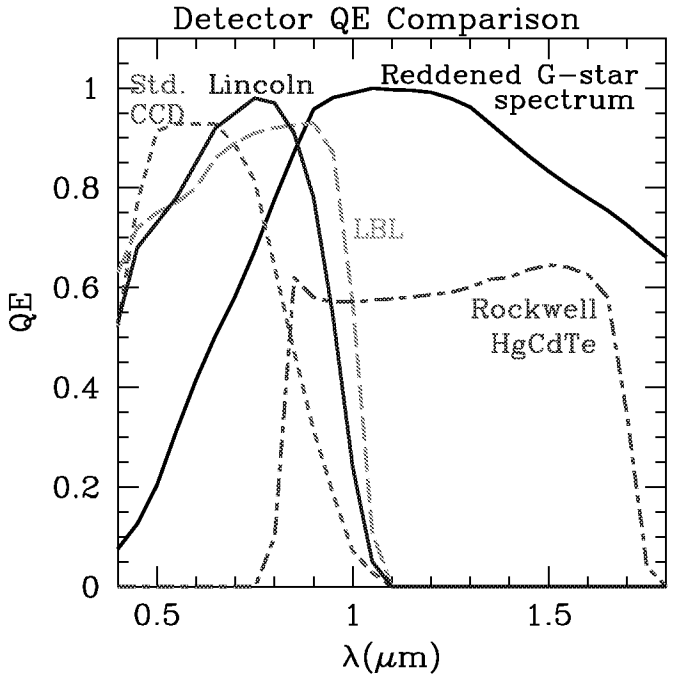

FIG. 2.—Spectrum of a typical reddened, Galactic bulge source star compared to the quantum efficiency curves for detectors that might be used for a microlensing planet search program. The standard CCD curve represents a Marconi CCD, which has a QE curve similar to the CCDs that are currently being produced by Fairchild and SITe as well as Marconi. The Lincoln Labs and LBL CCDs use high-resistivity silicon for enhanced sensitivity in the near-IR, and the Rockwell device is one designed for *HST*'s upcoming Wide Field Camera 3. [*See the electronic edition of the Journal for a color version of this figure.*]

sensitivity improvements of 44%, 62%, and 150% for the Lincoln, LBL, and Rockwell detectors, respectively, when compared to the sensitivity of the standard astronomical CCD. At the time of this writing, only the standard and Lincoln CCDs can be produced in the large quantities needed for a microlensing planet search mission, but this situation may change in the near future.

It is anticipated that *GEST* and *STEP* will take ~100 s exposures at 2 minute intervals, which would be co-added into 10 minute exposures. Assuming digitization at 14 bits pixel^{-1}, this gives a total data rate of 14 Mbits s^{-1} if no data compression is employed.

In order to make use of the high angular resolution available from space, it is necessary for the space-based telescope to have high pointing stability. We require that the pointing be stable to 10% or better of the assumed 0.″2 CCD pixel size. This should be achievable with three-axis stabilized, ultralow jitter spacecraft, such as Lockheed's LM-900, as long as a fine-guidance signal is provided from guide CCDs in the science focal plane, which would be read out a few times per second. Another option, which could correct higher frequency pointing jitter, would be to use a fast-guiding secondary mirror. The only pointing variation needed during the ~8 month Galactic bulge season would be a subpixel scale dither pattern needed to ensure that the photometric accuracy remains very close to the photon noise limit (Lauer 1999; Gilliland et al. 2000).

In this paper, we present the results of a detailed simulation of a space-based microlensing planet search mission. In § 2, we explain the assumptions and the details of our simulation and argue that our assumptions are conservative. In § 3, we present the details of our results including example light curves, the predicted planet detection sensitivity to bound and free-floating planets, and the prospects for direct observations of the lens stars. There is also a brief discussion of the ~50,000 planets that such a mission is likely to detect via transits. Finally, in § 4, we summarize the scientific results to be expected from a space-based microlensing planet search mission.

2. MISSION SIMULATION DETAILS

In order to simulate a space-based microlensing planet search mission, we must make assumptions regarding the source stars, the lens star systems, and the telescope. Our distribution of source stars is based on the Galactic bulge luminosity function of Holtzman et al. (1998). Following the *GEST* proposal, we select a field at Galactic coordinates $l \approx 1.^\circ2$, $b \approx -2.^\circ4$, which is closer to the Galactic center than the Baade's window field observed by Holtzman et al. This implies that both the star density and the reddening will be higher, and we split the field into two pieces for the purposes or our simulations in order to account for the gradient of the star density with Galactic latitude. The two half-fields have central Galactic latitudes of $b = -2.^\circ0$ and $-2.^\circ8$, and we have assigned them star densities of 2.06 and 1.55 times the Holtzman et al. (1998) star density measured at $b = -3.^\circ9$ based on number counts of "red clump" stars in the MACHO fields (Popowski et al. 2001). The *I*-band extinctions for these two half-fields are assumed to be $A_I = 1.6$ for the inner half-field and $A_I = 1.5$ for the outer half-field. These reddening values can be obtained from the Schlegel, Finkbeiner, & Davis (1998) dust map with a correction for stellar emission as advocated by Stanek (1999) or by assuming that the excess IR emission is proportional to the red clump star number counts.

Another very crucial physical input for our simulation is the microlensing probability (or optical depth, τ) toward the Galactic bulge. Measured values are $\tau = (3.3 \pm 1.2) \times 10^{-6}$ at $l = 0.^\circ9$, $b = -3.^\circ8$ (Udalski et al. 1994), $\tau = 3.9^{+1.8}_{-1.2} \times 10^{-6}$ at $l = 2.^\circ55$, $b = -3.^\circ64$ (Alcock et al. 1997), and $\tau = 3.23^{+0.52}_{0.50} \times 10^{-6}$ at $l = 2.^\circ68$, $b = -3.^\circ35$ (Alcock et al. 2000b). We have used this latest measurement because it is based on the largest sample, and it is closest to the theoretical estimates. Theoretical determinations of the scaling of the microlensing probability with position (Bissantz et al. 1997; Peale 1998) indicate that the microlensing probability at *GEST*'s outer half-field ($l = 1.^\circ2$, $b = -2.^\circ8$) should be 1.2–1.3 times larger than at $l = 2.^\circ68$, $b = -3.^\circ35$, while the increase at the inner half-field ($l = 1.^\circ2$, $b = -2.^\circ0$) should be a factor 1.4–1.8. For the purposes of this simulation, we have selected a conservative choice for the microlensing probability, $\tau = 2.43 \times 10^{-6}$ at $l = 2.^\circ68$, $b = -3.^\circ35$, which we then scale to $\tau = 2.9 \times 10^{-6}$ at $l = 1.^\circ2$, $b = -2.^\circ8$ and $\tau = 3.9 \times 10^{-6}$ at $l = 1.^\circ2$, $b = -2.^\circ0$. This is the 1.6 σ lower limit on the value of τ extrapolated to our selected field.

The mass function of the lens stars is assumed to follow the a conventional power-law form, $f(m) \propto m^{-\alpha}$, where $f(m)dm$ is the number of stars in the mass interval m to $m + dm$. We use a mass function similar to those advocated by Zoccali (2000) and Kroupa (2000), which implies different values of α in different mass intervals: $\alpha = 2.3$ for $m > 0.8\ M_\odot$, $\alpha = 1.33$ for $0.15\ M_\odot < m < 0.8\ M_\odot$, and $\alpha = 0.3$ for $0.05\ M_\odot < m < 0.15\ M_\odot$. The mass function is

truncated at 0.05 $M_\odot$ in order to keep the distribution of microlensing event timescales consistent with the observations of Alcock et al. (2000b). Stellar remnants are also included with white dwarfs contributing 13% of the lens stars, while neutron stars and black holes contribute less than 1% and less than 0.1% of the lens stars, respectively.

With these parameters for the properties of the inner Galaxy, we precede to run our simulations as follows:

1. We create an artificial image with stars $0 \leq M_I \leq 9$ at random locations in an artificial image using a "pseudo-Gaussian" profile (as in DoPHOT; Schechter, Mateo, & Saha 1993) with an FWHM of 0".24. Brighter stars are not included, but we assume that 5% of the 2.1 deg^2 field of view is lost because of bright, saturated stars or CCD defects.
2. A stellar lensing event is selected for each star in the frame with lens parameters selected at random assuming the mass function described above and a density and velocity distribution from a standard model of the Galaxy (Han & Gould 1997). All stellar lensing events are assumed to have an impact parameter of ≤ 3 Einstein radii, and the source stars are assumed to reside at 0.5 kpc behind the Galactic center, which is at $R_0 = 8$ kpc.
3. The orientation of each "exoecliptic" plane is selected at random, and then planet locations are selected by assigning each planet a random orbital phase within this plane. The planets are assumed to follow circular orbits with radii between 0.25 and 30 AU and mass fractions ranging from $\epsilon = 3 \times 10^{-7}$ to $\epsilon = 10^{-3}$.
4. Planetary lensing light curves are constructed assuming measurements every 10 minutes. Finite source effects are incorporated assuming a mass-radius relationship taken from Bertelli et al. (1994).
5. The CCD camera is assumed to detect 13 photons s^{-1} from an $I = 22$ star. This can be achieved with a 1.5 m telescope with standard CCDs employing a 650–900 nm passband or with a 1.0 m telescope with high-resistivity Lincoln Labs or LBL CCDs with a 500–1000 nm passband.
6. Light-curve error bars are generated under the assumption that the photometric accuracy is limited by photon statistics for noise levels down to 0.3%. This level of accuracy has been demonstrated with highly undersampled *HST* images of very crowded star fields (Lauer 1999; Gilliland et al. 2000). The key to this photometric accuracy is to recover the diffraction-limited resolution with a subpixel scale dither pattern. The undersampling of these *HST* images is similar to the level of undersampling for the proposed *GEST* mission, as shown in Figure 1. In addition to the source star, the lens star and nearby stars with images that are blended with the source star are assumed to contribute to the photon noise.
7. A single-lens, point-source light curve is fitted to each event, and planet detections are signaled by an excess fit χ^2. We measure the planetary signal with the $\Delta\chi^2$ that is the difference between the χ^2 for the single-lens fit and the correct planetary lensing fit. Our detection threshold is $\Delta\chi^2 \geq 160$, which is the equivalent of a 12.5 σ detection.

One potential drawback with our method for identifying planet detections is that planet detections may be incorrectly indicated for events with very high magnification because the effects of the finite angular size of the source star may be seen. These high-magnification events also have higher sensitivity to planets than lower magnification events (Griest & Safizadeh 1998; Rhie et al. 2000a) because the source star must necessarily pass close to the "stellar" caustic curve, which will be distorted because of the presence of planets. However, the determination of the planetary mass fraction (ϵ) and separation can be difficult for events detected because of the stellar caustic (Dominik 1999). Thus, it is not yet clear how useful such detections will be, although they do present enhanced sensitivity to multiple planets (Gaudi, Naber, & Sackett 1998). Because of this uncertainty, we have excluded planets detected in events with maximum magnifications greater than 200.

3. EXPECTED RESULTS

3.1. *Planetary Parameters from Microlensing*

The diversity of microlensing planetary light curves has been studied quite extensively (Mao & Paczyński 1991; Gould & Loeb 1992; Bolatto & Falco 1994; Bennett & Rhie 1996; Wambsganss 1997; Gaudi & Gould 1997; Gaudi 1998), and these studies have shown that it is possible to measure both the planetary mass fraction ϵ and the planet-star separation from the light-curve shape. The duration of the planetary light-curve deviation gives ϵ. The overall magnification of the light curve at the time of the planetary deviation and the basic shape of the planetary deviation give the separation. However, the transverse separation a is only determined in units of the Einstein ring radius,

$$R_{\rm E} = 2.85 \text{ AU} \sqrt{\frac{M_{\rm lens}}{M_\odot} \frac{D}{1 \text{ kpc}}}, \quad (1)$$

which is just the radius of the ring image for a single lens of mass $M_{\rm lens}$ that is perfectly aligned with the source star. $D = D_l(D_s - D_l)/D_s$, where D_l and D_s are the distances to the lens and source stars, respectively.

For a source star in the Galactic bulge, $R_{\rm E}$ is typically ~ 2 AU, and it ranges from 1 to 4 AU, so a measurement of $a/R_{\rm E}$ will yield an estimate of a that is good to a factor of 2. For most of the terrestrial planet detections, however, we can do somewhat better than this because we can also measure the time for the lens center of mass to cross the source star radius, t_s. This parameter is measurable for events in which the source comes very close to or crosses one of the lens caustics. This occurs for a large fraction of the terrestrial planet events, but there are many of the giant planet lensing events that are detectable without a close approach to a caustic. Precise values of a and $M_{\rm lens}$ can be obtained for events in which the lens can be detected via either multicolor photometry, spectroscopy, or proper motion as the lens separates from the source in the years after the event. This should be possible for about one-third of the events including virtually all of the F, G, and K star lenses (see § 3.7 for a more detailed discussion of source star identification).

3.2. *Event Light Curves*

Examples of the planetary light curves from our *GEST* mission simulation are shown in Figures 3–5. The data are shown with the error bars determined as described above, and the light curves are presented with the sampling interval of 10 minutes that was used for the event detection calculations. While the error bars are meant to indicate the 1 σ uncertainties, we have not added this noise to the data points shown in Figures 3 and 4 because of the high density

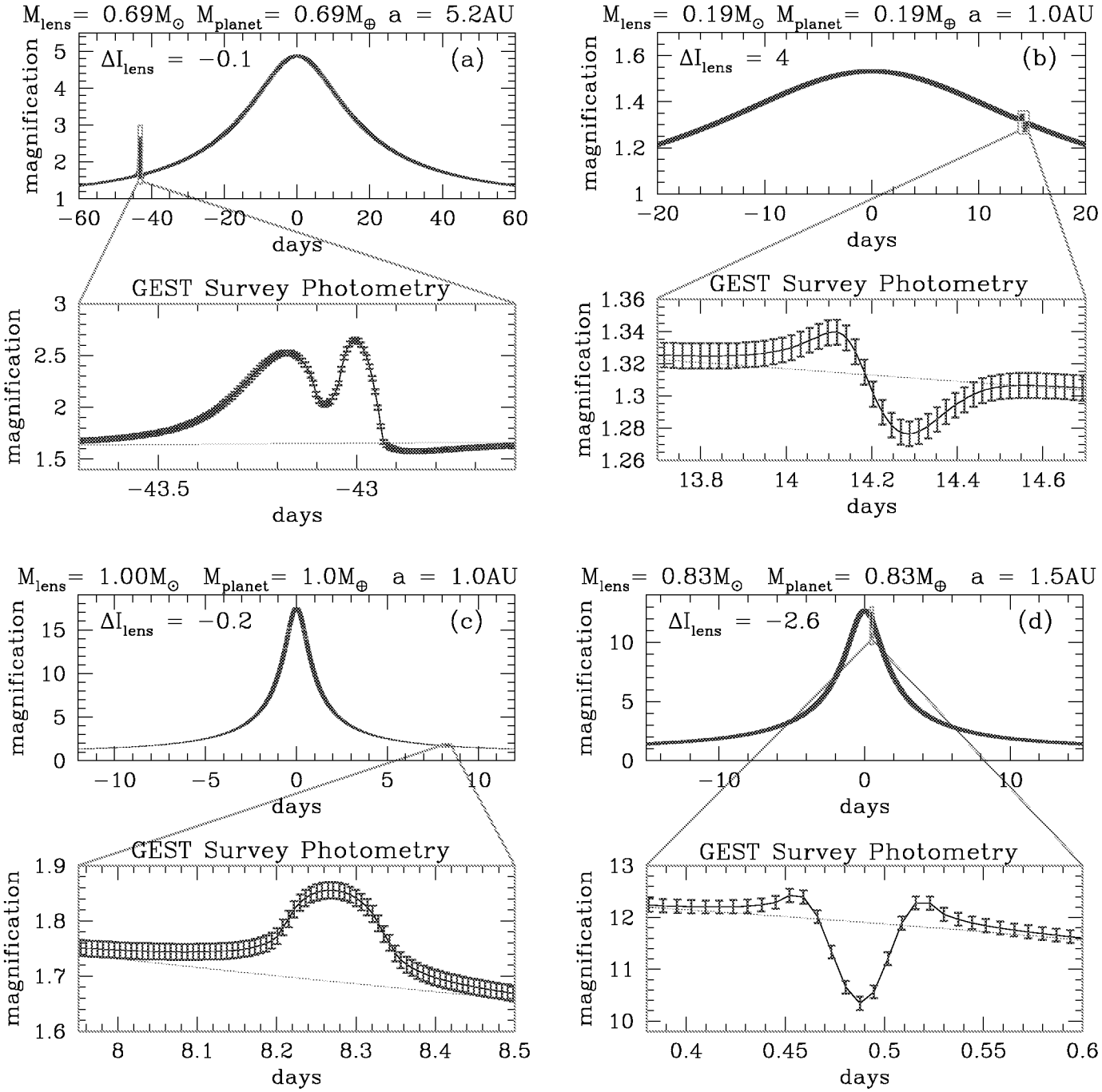

FIG. 3.—Example light curves shown from a simulation of the *GEST* mission. In each case, the top panel shows the full light curve, and the planetary deviation regions are blown up and shown in the lower panels. All of the example light curves have the Earth : Sun mass ratio of $\epsilon = 3 \times 10^{-6}$. Panels (*a*) and (*b*) span the range of planetary detection significance from (*a*) $\Delta\chi^2 = 60{,}000$ to (*b*) $\Delta\chi^2 = 180$, which is close to our cut. Panels (*c*) and (*d*) show more typical light curves with $\Delta\chi^2 = 3000$ and $\Delta\chi^2 = 500$, respectively. The planets detected in (*b*) and (*c*) have orbital radii of 1 AU, while the events shown in (*a*) and (*d*) have orbital radii of 5 and 1.5 AU, respectively. $\Delta I_{\rm lens}$ is the difference between lens and source *I* magnitude. [*See the electronic edition of the Journal for a color version of this figure.*]

of data points in these figures. These light curves are meant to illustrate the range of planetary light curves that a space-based microlensing survey should detect. They also represent the range of signal-to-noise ratios of the terrestrial planet detections in our *GEST* simulations. Figure 3*a* represents one of the highest signal-to-noise planet detections with the Earth : Sun mass ratio of $\epsilon = 3 \times 10^{-6}$, and Figure 3*b* is an event that barely passes our event detection cut of $\Delta\chi^2 \geq 160$. The other events have more typical signal-to-noise ratios.

We have assumed that the photometric accuracy of a space-based microlensing survey will be dominated by photon statistics and that systematic errors will not become dominant until the statistical errors reach less than 0.3% (in five co-added 100 s exposures). However, Figures 3 and 4 illustrate that most of the planet detections are made with

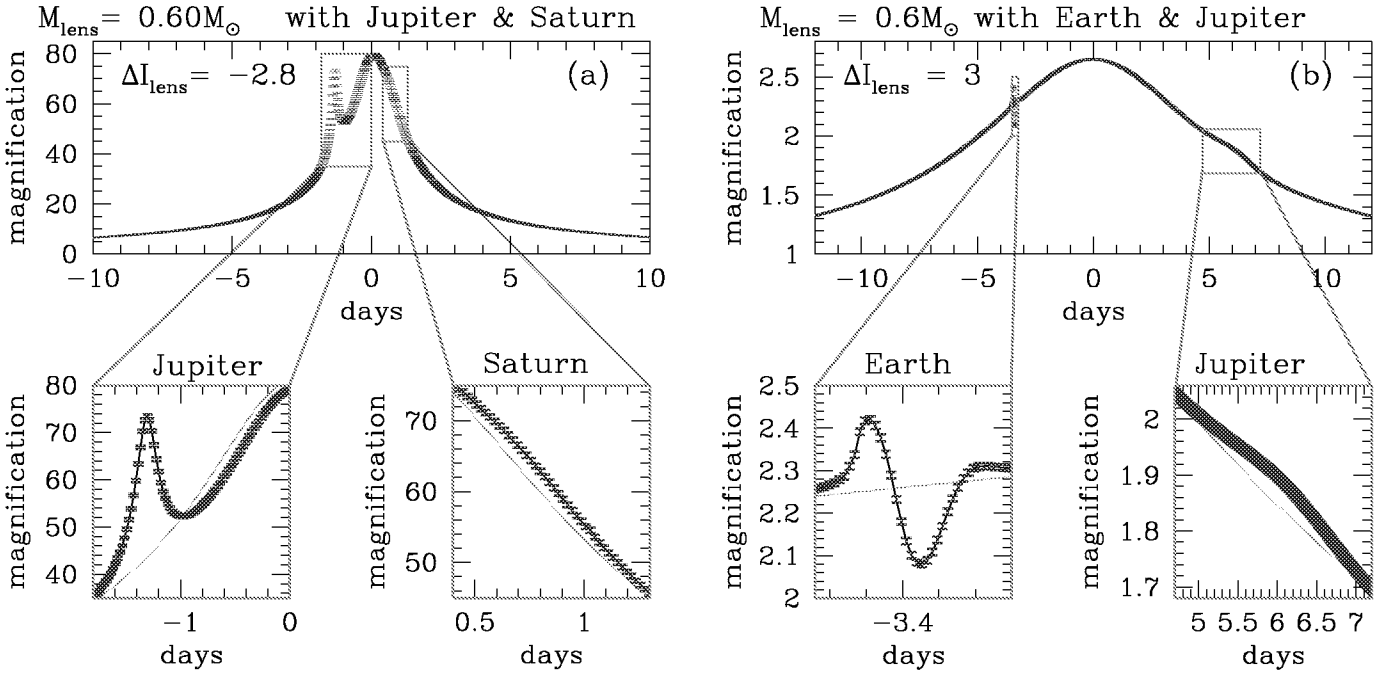

FIG. 4.—Example multiple-planet light curves from our simulation of planetary systems with the same planetary mass ratios and separations as in our solar system. Panel (*a*) is an example of a Jupiter/Saturn detections, and panel (*b*) is an example of the detection of Earth and a Jupiter. [*See the electronic edition of the Journal for a color version of this figure.*]

lower precision photometry, with photometric errors of ~1% dominated by photon statistics.

These events serve to illustrate why ground-based microlensing searches are not effective for the detection of terrestrial planets (Bennett & Rhie 2000a, Rhie et al. 2000b[8]). The necessity of using main-sequence target stars for a microlensing program to find terrestrial planets means that the accuracy of photometry is compromised by the blending of the source star images as demonstrated in Figure 1. This is true even if the planet search program is limited to the best ground-based observing sites such as Paranal (Sackett 1999). This blending with neighboring stars less than an arcsecond away substantially reduces the photometric signal-to-noise ratio and would make the events shown in Figures 3*b*–3*d* undetectable. The event shown in Figure 3*a* would have a large enough signal to be detectable from a ground-based program, but since the planetary deviation lasts for more than 24 hr, it would be poorly sampled from a single site. Follow-up observations from sites at other longitudes would be of little help because the poorer seeing at these sites would make the photometry too noisy to be very useful in characterizing the properties of the detected planet.

3.2.1. *Light Curves for Multiple Planets and Moons*

Figure 4 shows events in which multiple planets are detected. Most multiple-planet events have light curves that are very similar to single-planet events except that there are two different planetary deviation regions. We have run simulations of "solar-type" planetary systems in which every stellar lens is assumed to have planets with the same mass fractions as the planets in the solar system and with the same separations. Most of the multiple-planet detections in our simulations are similar to Figure 4*a*, in which both the "Jupiter" and "Saturn" planets are detected. In about 25% of the cases where the Saturn planet is detected, the Jupiter planet is also detected. This is a consequence of the fact that Saturn's orbital semimajor axis is only a factor of 1.8 larger than Jupiter's orbital semimajor axis. Such orbits are stable only if they are close to circular, so a space-based microlensing survey will be able to provide information on the abundance of giant planets with nearly circular orbits by measuring the frequency of double-planet detections and the ratios of their separations. This is important information since giant planets in Jupiter- or Saturn-like orbits are thought to be required for the delivery of volatiles, such as water, to the inner planets in the habitable zone (Lunine 2001).

Events in which a terrestrial planet and a Jupiter planet are detected, such as the event shown in Figure 4*b*, are more rare. In part, this is because the lower mass of the terrestrial planet means that less of them will be detected, but another factor is that the ratio of Jupiter's semimajor axis to that of the terrestrial planets is a factor of 3.5–7 rather than the factor of 1.8 ratio between the Jupiter and Saturn orbital distances. Because of this, only 10%–15% of the detected terrestrial planets will also have a Jupiter detection.

The detection sensitivity for multiple planets depends more on the telescope size and the assumed level of systematic photometry errors than the sensitivity for single planets does. More sensitive photometry increases the probability that a planet can be detected in the light curve of a microlensing event, and the number of double planets detected depends on this probability squared.

In order to estimate the sensitivity for detecting multiple planets, we have calculated the detection probabilities for lenses with planetary systems with the same planetary mass fractions and separations as the planets of our own solar system. For the parameters of the proposed *GEST* mission, we find that a total of about 150*f* multiple-planet systems

[8] See footnote 3.

will be discovered, where f is the fraction of planetary systems that resemble our own. About $13f$ of these will be terrestrial giant planet pairs, and the remainder will be multiple-planet detections consisting of only giant planets. (These numbers assume that a lower detection threshold of 9σ can be used for the second planets to be detected because there is a much smaller number of light curves that must be searched for multiple planets.) A substantial improvement in sensitivity can be obtained with the parameters of the *STEP* mission: a 1.5 m telescope with a 2.2 deg^2 field of view. Half of the focal plane would use Lincoln Labs near-IR optimized CCD detectors, and the other half would use the HgCdTe IR arrays with a 1.7 μm cutoff. If we assume that the photometry is limited by systematic errors of 0.15% in a 10 minute exposure, then our simulation indicates a total of $490f$ multiple-planet detections with $45f$ of these being terrestrial giant planet pairs.

It is also possible to detect the large moons of terrestrial planets as shown in Figure 5. The semimajor axis of the Moon's orbit is about 0.8 times the Earth's Einstein radius, so systems like our own should be detectable. Because the planet-moon separation is likely to be similar to the planetary Einstein radius, the light-curve deviations due to the planet and moon are likely to be closely spaced in time or even overlapping, as in the example shown in Figure 5*b*. Nevertheless, most of the light-curve deviations due to planet+moon systems are well approximated by the sum of the deviations due to the two minor masses by themselves. A more systematic study of the detection of planet+moon systems by microlensing will be carried out in a future paper.

3.3. *Planet Detection Sensitivity*

The major goal of our simulations is to determine the sensitivity of a space-based microlensing survey. The sensitivity to planets orbiting each of the lens stars depends on a large number of factors including the event timescale, the size of the photometric error bars, and the angular size of the source star. Thus, the simplest way to display the planet detection sensitivity is to give the number of expected planet detections under the assumption that each lens star has a planet of a given mass fraction ϵ and separation. This is what is plotted in Figures 6 and 7. The different curves in Figure 6 are contours of constant numbers of planet discoveries, assuming one planet per star at the given mass fraction and semimajor axis. In Figure 7, we compare the sensitivities of the proposed *GEST* and *STEP* missions. The locations of the planets in our solar system are also shown. Each planet name starts at the planetary mass fraction of the planet and continues toward higher mass fractions. Because the typical mass of a lens star is about 0.3 $M_\odot$, planets of the same mass as the solar system's planets will have a typical mass fraction that is larger by about a factor of 3. A planet of one Earth mass, for example, will usually have $\epsilon \approx 10^{-5}$ rather than $\epsilon = 3 \times 10^{-6}$, which is the Earth's mass fraction. So, the sensitivity to planets with the same mass as those in the solar system will appear near the top of each planet name, while the bottom of each planet name indicates the sensitivity to planets of a fixed mass fraction. The sensitivity to planets of 1 $M_\oplus$ for the parameters of the *GEST* mission is shown in Figure 8, which indicates that just over 100 Earths would be detected if each lens star has one in a 1 AU orbit. The peak sensitivity is at an orbital distance of 2.5 AU, where we would expect 230 detections if each lens star had a planet in such an orbit.

The shaded regions in Figure 6 indicate the sensitivity of other planet search techniques. The known extrasolar planets that orbit main-sequence stars have been discovered with the precision radial velocity technique (Marcy & Butler 1996), and a number of these individual detections are indicated in the upper left-hand region of the figure at small semimajor axes and large masses. The solid, faint shaded

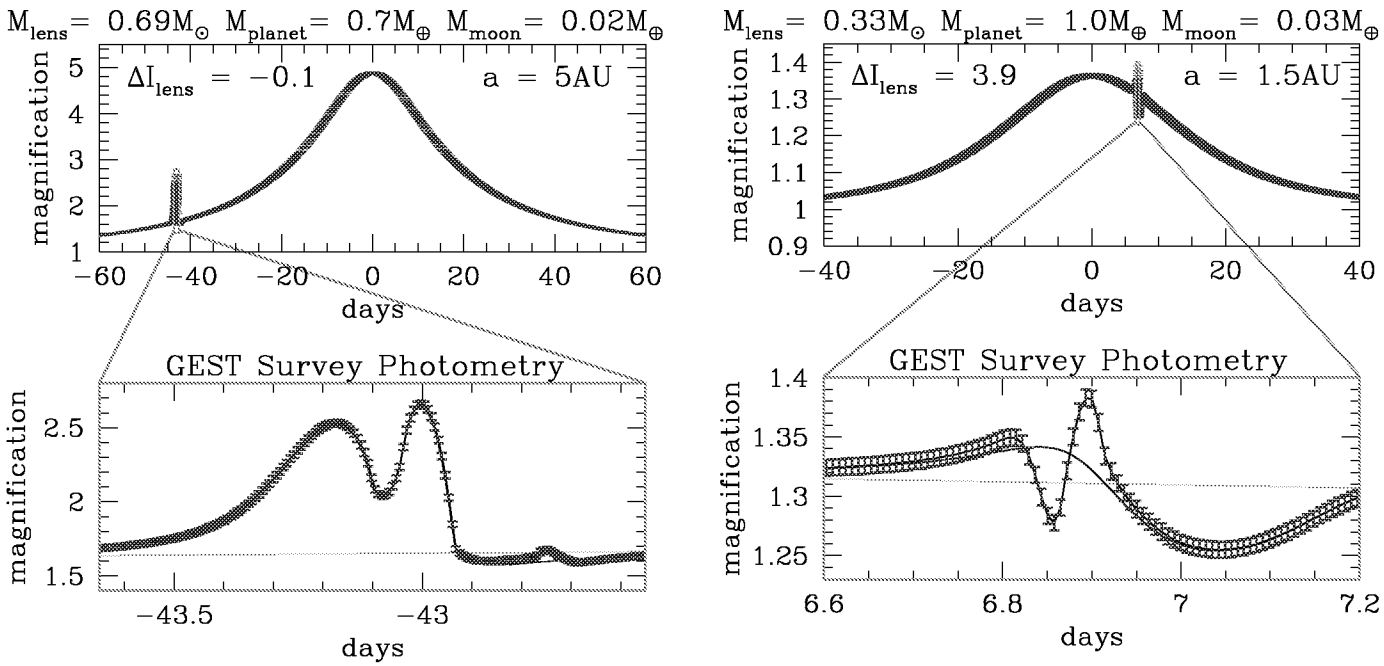

FIG. 5.—Example light curves of terrestrial planets with moons that have 1–2 times the mass of the Earth's Moon. These moons orbit at 3.3 and 0.56 times the Earth-Moon separation, respectively. [*See the electronic edition of the Journal for a color version of this figure.*]

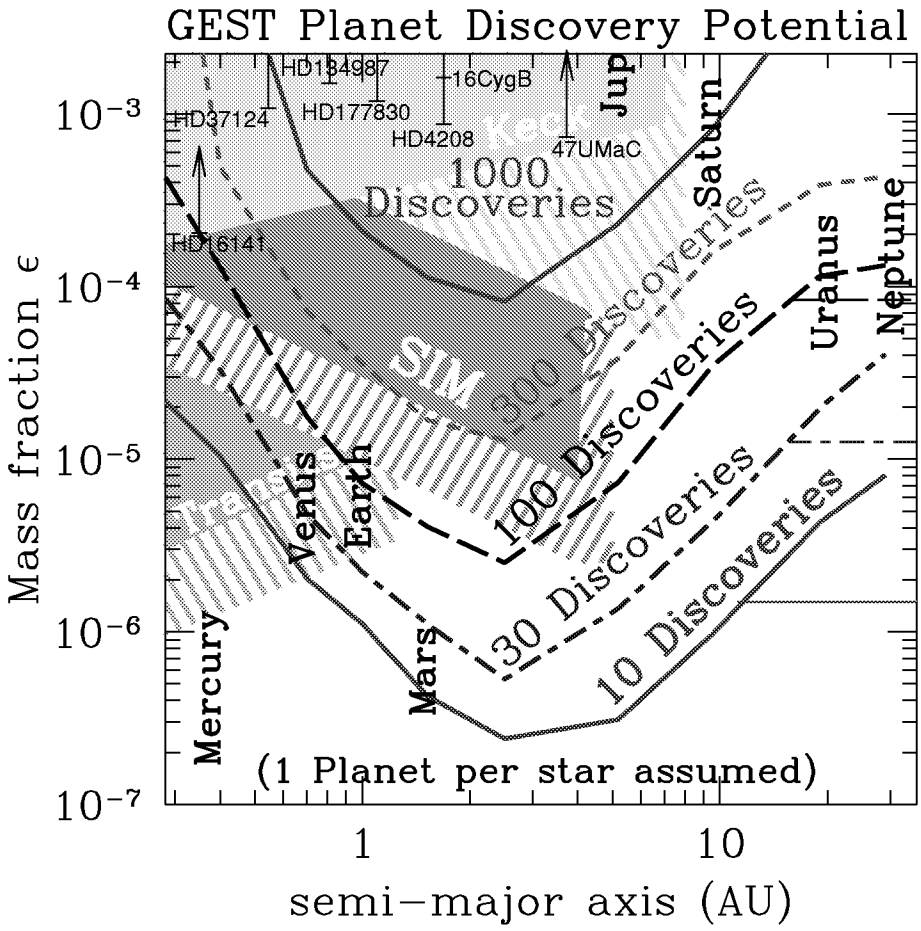

FIG. 6.—Sensitivity of the proposed *GEST* mission plotted as a function of planetary mass fraction ϵ and orbital semimajor axis. The curves are contours indicating the expected number of *GEST* planet discoveries assuming one planet per star with the given parameters. The faint solid region gives the sensitivity of a 20 yr radial velocity program on the Keck Telescope assuming a detection threshold of 10 m s^{-1}, and the faint lines indicate the sensitivity of a 10 yr interferometric astrometry program with a 30 μas detection threshold. The sensitivity of the *SIM* recommended and floor missions are indicated. The location of our solar system's planets and some of the extrasolar planets detected by radial velocities are shown. Most detected Earth mass planets have $\epsilon \approx 10^{-5}$ because the typical lens star has a mass of $\sim$0.3 $M_\odot$, so the plot indicates that *GEST* can see $\sim$35 Earth mass ratio planets at 1 AU and $\sim$100 Earth mass planets at that distance. The horizontal lines indicate the sensitivity to free-floating planets since the more distant planets can sometimes be detected without seeing a microlensing signal from their star. [*See the electronic edition of the Journal for a color version of this figure.*]

region indicates the sensitivity of a 20 yr radial velocity program assuming a minimum detectable velocity amplitude of 10 m s^{-1}. This is close to the demonstrated accuracy of the Keck (Marcy & Butler 1996) and CORALIE (Queloz et al. 2000) radial velocity programs, but it is expected that the current radial velocity state-of-the-art measurements are close to the limit set by the intrinsic radial velocity noise of the source stars. The expected sensitivity of the planned 5 yr *SIM* satellite is shown with the vertical lines showing the planned *SIM* sensitivity and the solid shaded region showing the sensitivity of the *SIM* floor mission. (The assumed detectable astrometric signals are 1 and 6 μas, at a distance of 10 pc.)

The shaded region near 10^{-5} on the left-hand side of Figure 6 represents the space-based transit technique, which is very sensitive to terrestrial planets in short-period orbits. Several such transit missions are planned, including the French *COROT* mission, ESA's (not yet funded) *Eddington* mission, and NASA's *Kepler* mission. *Kepler* will be the most sensitive of these, and its sensitivity is represented by the diagonal lines extending downward. A sensitive transit search like *Kepler* is the only program that is competitive with a space-based microlensing survey for finding Earth mass planets at 1 AU. However, the prime sensitivity of a transit survey extends inward from 1 AU, while the sensitivity of microlensing extends outward. So, the two methods are largely complementary.

Figure 6 indicates that microlensing's peak planet detection sensitivity is at 2–3 AU with significant sensitivity in the range 0.7–10 AU. In fact, the sensitivity at large distances is underestimated by our simulation because we do not consider planets that may be detected when the source star magnification is $A < 1.06$. Events with $A_{\max} < 1.06$ and events with the planetary deviation that occurs before or after the $A > 1.06$ region of the light curve have not been included in our simulations. However, some of these planets will be detectable. A lower limit on our sensitivity to distant planets is set by our sensitivity to free-floating planets, which is discussed in § 3.6. This sensitivity is indicated by the thinner, horizontal lines on the right-hand side of Figure 6. These lines should be considered to extend to infinite distances, indicating that a space-based microlensing survey has strong sensitivity to planets at separations of 0.7 AU to ∞. However, for planets at distances $\gg 10$ AU, it will often be

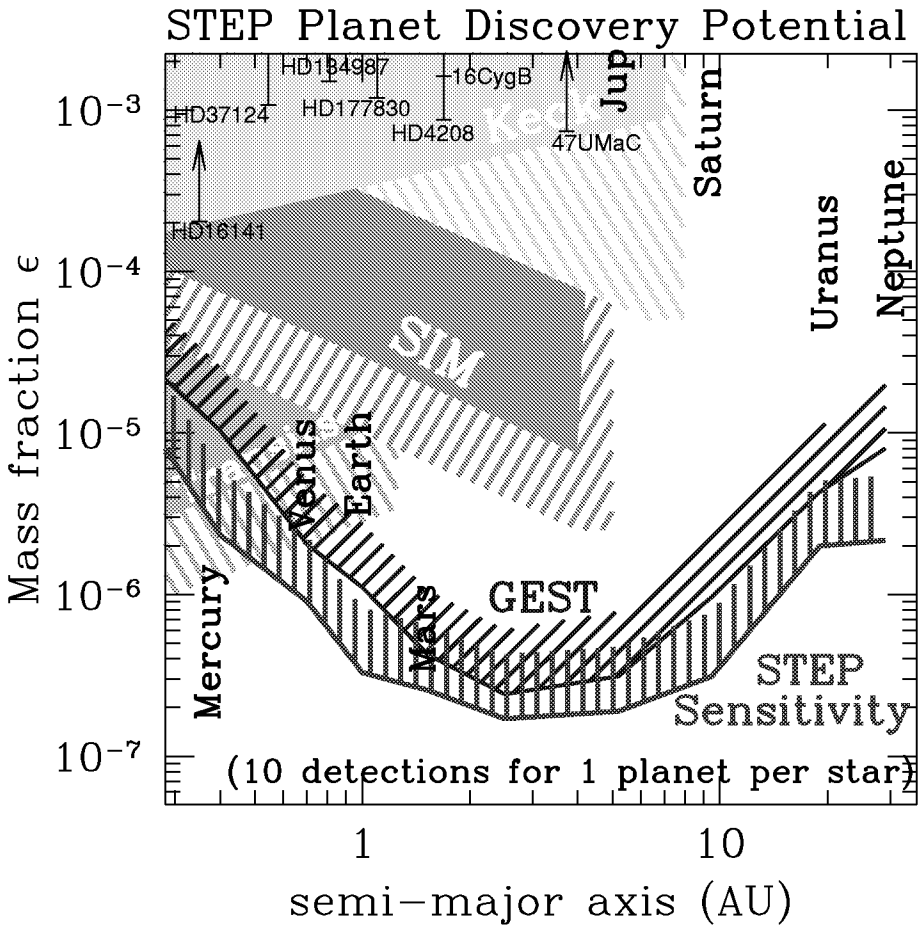

FIG. 7.—Sensitivity of the more ambitious *STEP* mission compared to the sensitivity of the proposed *GEST* mission, as well as the other planet search techniques shown in Fig. 6. The improvement in sensitivity due to *STEP*'s larger telescope and more sensitive detectors is more pronounced at large and small separations than at the region of maximum sensitivity at 2–3 AU. This is because the more sensitive mission is able to detect planetary signals of a smaller amplitude that often occur for planets with separations that are significantly smaller or larger than the Einstein ring radius. [*See the electronic edition of the Journal for a color version of this figure.*]

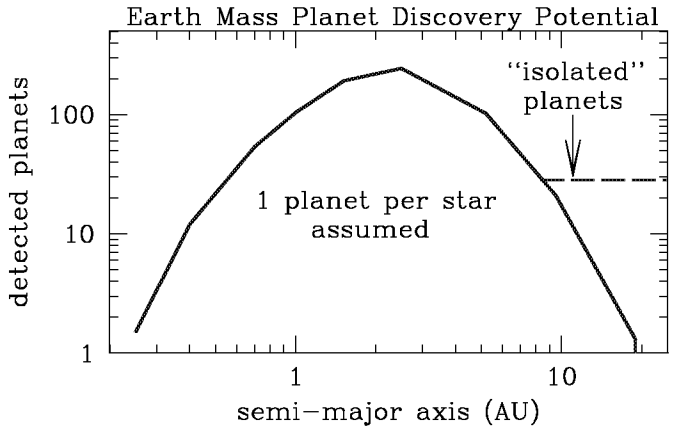

FIG. 8.—Plot of *GEST*'s sensitivity to Earth mass planets. The number of detected Earth mass planets is shown as a function of the orbital semimajor axis assuming one such planet per lens star. At a semimajor axis of ~10 AU, the number of planet detections reaches the lower limit of about 30 set by the free-floating planet detection calculation. Most of the planets detected with semimajor axis $\gg 10$ AU will be detected in "isolation," without a detection of their host star. [*See the electronic edition of the Journal for a color version of this figure.*]

the case that the star that the planet orbits will not be detectable. Such cases may be difficult to distinguish from free-floating planet detections unless the lens star can be detected (see § 3.7).

Microlensing of Galactic bulge stars is most sensitive at semimajor axes of 2–3 AU because this is the typical Einstein ring radius for Galactic bulge source stars. Images are located close to the Einstein ring when they are bright, and the planet is most easily detectable if one of the bright images passes close to it. In contrast, the astrometry technique is more sensitive at large orbital radii, while the radial velocity and transit techniques (see § 3.9) are more sensitive at smaller radii. The astrometry, radial velocity, and transit techniques all have sharp cutoffs on their sensitivity at larger semimajor axes because of the fact that these techniques require data from a full orbit, or several orbits in the case of transits. Thus, microlensing has an advantage over these other techniques at large orbital distances since it is able to make prompt discoveries of distant planets.

The main advantage of the microlensing technique over both the astrometry and radial velocity techniques is its sensitivity to lower mass planets. At 1 AU, microlensing is sensitive to planets with masses that are about 3 orders of magnitude smaller than the smallest masses that ground-based radial velocity and astrometry searches are likely to

detect. A space-based microlensing survey also offers an advantage in sensitivity to low-mass planets with respect to space-based astrometry missions such as *SIM*. Figure 6 indicates that *GEST*'s sensitivity extends to masses that are a factor of 20 lower than expected for the *SIM* baseline mission and a factor of 100 lower than for the *SIM* floor mission. (The floor mission is considered to be the minimum acceptable sensitivity that *SIM* could descope to if it should run into budget problems.) Of course, *SIM* will find planets orbiting nearby stars, so planetary results to be expected from the *GEST* and *SIM* missions are somewhat complementary: *GEST* will determine extrasolar planet abundances extending down to very low masses, while *SIM* will study planetary systems close to the Sun with sensitivity down to planets somewhat more massive than the Earth.

Another important advantage of the gravitational microlensing technique is that the low-mass planets are detected with high signal-to-noise ratio. In fact, for a large range of planetary masses, the strength of the microlensing signal does not depend on the mass of the planet. Low-mass planets do affect a smaller region of the lens plane, so they have a lower detection probability and a shorter duration. Figure 9 shows the distribution of the signal-to-noise ratio of our detected planets for planetary mass fractions ranging from $\epsilon = 3 \times 10^{-7}$ (Mars-like) to $\epsilon = 3 \times 10^{-4}$ (Saturn-like). $\Delta\chi^2$ is the detection significance parameter used for the x-axis of this plot, and a logarithmic scale must be used because of the large spread in $\Delta\chi^2$ values. The most striking feature of this figure is that the number of events with large $\Delta\chi^2$ values falls off rather slowly. The power law, $N \sim (\Delta\chi^2)^{-1.3}$, provides a rough fit to these curves for all but the lowest mass fraction ($\epsilon = 3 \times 10^{-7}$), where the effects of the finite angular size of the source stars begin to reduce the number of high signal-to-noise ratio events.

3.4. *Sensitivity Dependence on Telescope Parameters*

Tables 1 and 2 summarize how the planet detection sensitivity for Earth-like planets depends on the parameters of the space-based microlensing survey telescope. The parameters varied are the telescope field of view, the assumed minimum photometric error in a 10 minute exposure, the assumed FWHM of the images, and the effective telescope aperture in meters. The FWHM and aperture are considered independently because they can be varied independently when the passband and telescope optics are varied. The passband and detector sensitivity contribute to the effective aperture by modifying the total number of photons detected. The effective aperture is normalized assuming the detector quantum efficiency of the standard CCDs shown in Figure 2 with a broad 0.5–0.9 μm passband and a telescope optical throughput of 70%. Narrower passbands can decrease the effective aperture, and the use of more sensitive detectors can increase the effective aperture. Thus, the tele-

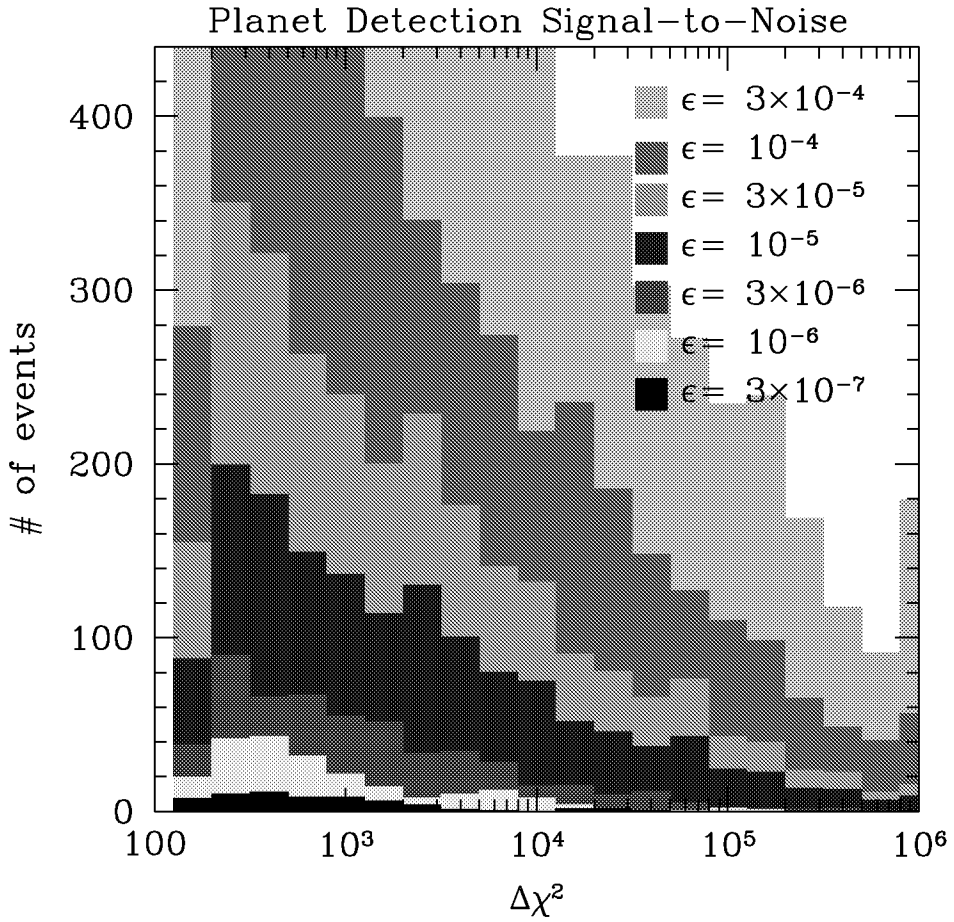

FIG. 9.—Histogram of the planetary detection significance $\Delta\chi^2$ for different mass fractions ϵ ranging from $\epsilon = 3 \times 10^{-7}$ (the mass fraction of Mars) to $\epsilon = 3 \times 10^{-4}$ (the mass fraction of Saturn). For planets with an Earth-like mass fraction ($\epsilon = 3 \times 10^{-6}$) and above, more than half of the detected events have $\Delta\chi^2 > 800$, which corresponds to a 28 σ detection. [*See the electronic edition of the Journal for a color version of this figure.*]

TABLE 1

TERRESTRIAL PLANET DETECTION SENSITIVITY FOR $\epsilon = 3 \times 10^{-6}$ AT 0.7–1.5 AU

ϵ	FOV (deg^2)	MINIMUM ERROR (%)	FWHM (arcsec)	EFFECTIVE TELESCOPE APERTURE (m)			
				1.0	1.25*	1.6	2.0
3×10^{-6}.....	1.5	0.3	0.32	0.612	0.759	0.921	1.049
3×10^{-6}.....	2.0	0.3	0.32	0.726	0.908	1.058	1.251
3×10^{-6}.....	2.5	0.3	0.32	0.839	1.058	1.281	1.454
3×10^{-6}.....	1.5	0.15	0.32	0.652	0.813	1.006	1.167
3×10^{-6}.....	2.0	0.15	0.32	0.778	0.976	1.205	1.396
3×10^{-6}.....	2.5	0.15	0.32	0.905	1.138	1.405	1.625
3×10^{-6}.....	1.5	0.3	0.24	0.665	0.837	0.983	1.119
3×10^{-6}.....	2.0*	0.3*	0.24*	0.795	1.000*	1.179	1.336
3×10^{-6}.....	2.5	0.3	0.24	0.925	1.163	1.374	1.553
3×10^{-6}.....	1.5	0.15	0.24	0.704	0.889	1.071	1.251
3×10^{-6}.....	2.0	0.15	0.24	0.846	1.065	1.285	1.494
3×10^{-6}.....	2.5	0.15	0.24	0.988	1.241	1.499	1.737
3×10^{-6}.....	1.5	0.3	0.16	0.723	0.904	1.072	1.217
3×10^{-6}.....	2.0	0.3	0.16	0.865	1.079	1.278	1.448
3×10^{-6}.....	2.5	0.3	0.16	1.008	1.254	1.485	1.679
3×10^{-6}.....	1.5	0.15	0.16	0.763	0.956	1.152	1.331
3×10^{-6}.....	2.0	0.15	0.16	0.918	1.144	1.378	1.587
3×10^{-6}.....	2.5	0.15	0.16	1.073	1.332	1.604	1.844

NOTE.—This table shows the ratio of the number of terrestrial planet detections as a function of the telescope aperture, field of view (FOV), and effective point-spread function FWHM. The parameters of the *GEST* MIDEX proposal are indicated with asterisks.

scope proposed for the *GEST* MIDEX proposal has an effective aperture of 1.25 m even though the actual aperture is 1.0 m because the more sensitive Lincoln Labs CCDs are used with a 0.5–1.0 μm passband.

The planet detection sensitivity has a weaker dependence on a number of these parameters than might naively be expected. For example, the number of planets detected does not depend linearly on the field of view because we are able to select a field with a higher average microlensing optical depth when the field is smaller. Also, the dependence on the image FWHM is relatively weak because all of the values considered allow stars near the top of the bulge main sequence to be individually resolved. The sensitivity decreases quite substantially at FWHM $\gtrsim 0\farcs5$, however.

We should caution that the main advantage of a more sensitive telescope, like the proposed *STEP* mission, is the increased sensitivity to multiple-planet detections. As described in § 3.2.1, the proposed *STEP* mission should

TABLE 2

TERRESTRIAL PLANET DETECTION SENSITIVITY FOR $\epsilon = 10^{-5}$ AT 0.7–1.5 AU

ϵ	FOV (deg^2)	MINIMUM ERROR	FWHM	EFFECTIVE TELESCOPE APERTURE (m)			
				1.0	1.25*	1.6	2.0
10^{-5}	1.5	0.3	0.32	0.680	0.793	0.906	1.016
10^{-5}	2.0	0.3	0.32	0.803	0.937	1.074	1.202
10^{-5}	2.5	0.3	0.32	0.925	1.082	1.243	1.389
10^{-5}	1.5	0.15	0.32	0.709	0.834	0.974	1.114
10^{-5}	2.0	0.15	0.32	0.837	0.985	1.153	1.320
10^{-5}	2.5	0.15	0.32	0.965	1.136	1.322	1.526
10^{-5}	1.5	0.3	0.24	0.732	0.846	0.969	1.095
10^{-5}	2.0*	0.3*	0.24*	0.863	1.000*	1.148	1.296
10^{-5}	2.5	0.3	0.24	0.994	1.154	1.326	1.497
10^{-6}	1.5	0.15	0.24	0.758	0.885	1.034	1.190
10^{-5}	2.0	0.15	0.24	0.894	1.046	1.225	1.411
10^{-5}	2.5	0.15	0.24	1.031	1.207	1.415	1.632
10^{-5}	1.5	0.3	0.16	0.769	0.889	1.039	1.164
10^{-5}	2.0	0.3	0.16	0.906	1.049	1.230	1.372
10^{-5}	2.5	0.3	0.16	1.042	1.209	1.421	1.582
10^{-5}	1.5	0.15	0.16	0.794	0.928	1.101	1.256
10^{-5}	2.0	0.15	0.16	0.936	1.094	1.302	1.483
10^{-5}	2.5	0.15	0.16	1.078	1.261	1.504	1.712

NOTE.—This table shows the ratio of the number of terrestrial planet detections as a function of the telescope aperture, field of view (FOV), and effective point-spread function FWHM. The parameters of the *GEST* MIDEX proposal are indicated with asterisks.

expect to detect 3–3.5 times more multiple-planet systems than the proposed *GEST* mission would. Some of this increase in sensitivity to multiple planets is due to the fact that the probability of detecting two planets scales like the single-planet detection probability squared. However, when one planet is detected, it often has a separation that is close to the Einstein ring radius. Since a second planet is likely to have a separation that is not close to the Einstein ring radius, it will likely have a weaker than average signal. Thus, the ability to detect multiple planets is more sensitive to the telescope size and detector sensitivity than the square of the single-planet detection probability.

3.5. *Variable Star Background*

All of our simulations have implicitly assumed that there is no significant background of variable stars that might interfere with the detection of planets. Some justification for this is provided by the existing gravitational microlensing surveys, which have not seen a significant background of variable stars (Alcock et al. 1997, 2000b; Udalski et al. 2000). In fact, the most significant source of variability that might contaminate samples of gravitational microlensing events are background supernovae (Alcock et al. 2000c). However, the space-based microlensing program that we propose will use source stars that are fainter than the source stars used for the ground-based surveys. Faint flare stars (Lacy, Moffett, & Evans 1976) are of particular concern because they can have long quiescent phases with infrequent brightenings seen in broadband photometry. However, this broadband variability is generally seen in the blue or ultraviolet bands and is much less pronounced in the red and near-IR, where microlensing surveys would observe.

While the ground-based microlensing surveys follow relatively bright stars in the Galactic bulge and Large Magellanic Cloud, they also observe many thousands of intrinsically fainter stars in the foreground of these targets. None of the foreground stars observed by the MACHO collaboration have exhibited the sort of photometric variation that could be confused with a planetary microlensing deviation if, by chance, the intrinsic stellar photometric variation occurred during a stellar microlensing event. Since we expect about 10^4 stellar microlensing events, the statistics of the foreground stars observed by the ground-based surveys suggest that there should be no contamination of the planet sample due to variable stars. The data provided by a space-based survey will provide much more stringent constraints on possible variable star contamination, and we expect that the accurate measurements of the light-curve shape from a space-based survey will clearly distinguish between deviations due to microlensing and any intrinsic variability of the source star. It is likely that the variable star background will have a negligible effect on the sensitivity of a space-based gravitational microlensing planet search program.

3.6. *Free-floating Planets*

The leading theories of planet formation (Levison, Lisauer, & Duncan 1998; Perryman 2000) indicate that planets often do not stay in the same orbit where they formed. The migration of giant planets inward is thought to be necessary to explain the "hot Jupiter" planets discovered by the radial velocity planet searches, and the orbital distribution of Kuiper belt objects (Malhotra, Duncan, & Levison 2000) suggests that Neptune has migrated outward from its birth site. These migrations are likely to be due to the gravitational interactions of these giant planets with a large number of planetesimals in the protoplanetary disk. Many of these planetesimals are likely to be perturbed into highly elliptical orbits that will send them crashing into the Sun or ejecting them from the solar system, and it is expected that the most massive of these ejected objects will have a mass in the terrestrial planet range that should be detectable via microlensing.

The majority of known extrasolar giant planets in orbits of semimajor axis larger than 0.3 AU have relatively large orbital eccentricities, and this can be explained via gravitational scattering with other giant planets in the same system (Levison et al. 1998). A consequence of these interactions is that many of these giant planets will be ejected from their planetary system. Terrestrial planets, which are more easily ejected via two-body interactions, should also be ejected in large numbers. Thus, there are good theoretical reasons to believe that free-floating planets may be abundant as a by-product of the planetary formation process. If so, they can be detected via gravitational microlensing. Figure 10 shows the number of free-floating planet detections expected for the *GEST* mission under the assumption that there is one free-floating planet per Galactic star. The detection threshold is set higher for the free-floating planet detections because we must search $\sim 10^8$ light curves for free-floating planets, while we only need to search the $\sim 10^4$ detected stellar microlensing event light curves for evidence of bound planets. Since theory predicts that many stars may be ejected from the system during the planetary formation process, it may be reasonable to assume that there will be many more free-floating planets than the numbers indicated in Figure 10. If half of the star systems eject an average of 10 1 $M_\oplus$ planets each, then we would expect to detect more than 100. In fact, there has already been a possible detection of a free-floating planet in the MACHO data (Bennett et al. 1997).

3.7. *Source Star Identification*

The planets detected by the space-based microlensing survey orbit the lens stars which are in the foreground of the Galactic bulge source stars. The mass distribution of the

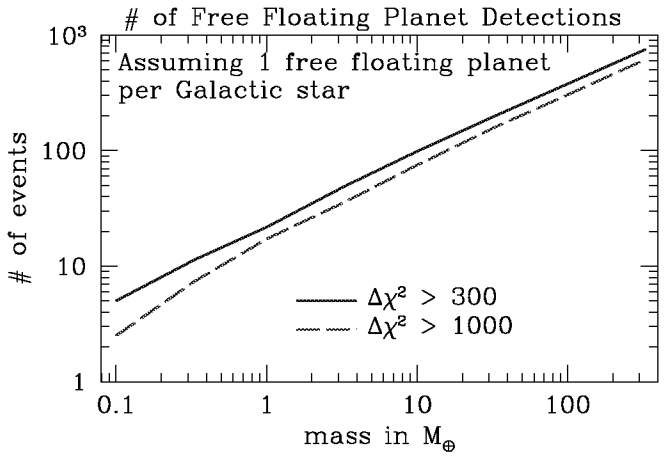

FIG. 10.—Number of free-floating planets to be discovered by *GEST* vs. planetary mass for two different detection criteria that are equivalent to 17 and 30 σ. [*See the electronic edition of the Journal for a color version of this figure.*]

lens stars from our *GEST* simulations is shown in Figure 11. This distribution is somewhat flatter than the stellar mass function because we have assumed that the planetary mass distribution is proportional to the stellar mass distribution and that more massive planets have a higher detection probability.

Although microlensing does not require the detection of any light from the lens stars, a significant fraction of the microlensing events seen by a space-based microlensing survey will have lens stars that are bright enough to be detected. Our simulations indicate that for ~17% of the detected planets, the planetary host (lens) star is brighter than the source star, and for another ~23%, the lens star is within 2.5 *I*-band magnitudes of the source star's brightness. A few of these stars are blended with the images of other brighter stars, and if we ignore those stars, we find that 33% of the lens stars should be directly detectable. The detectable planetary host stars are shown as the dark histogram in Figure 11, and they comprise virtually all of the F and G star lenses, most of the K star lenses, and a few of the nearby M star lenses.

The visibility of the lens star will allow for the measurement of a number of other useful parameters. The most obvious of these are the apparent magnitude and color of the lens star. This would enable an approximate determination of the lens mass and distance if the dust extinction was small. Our field, however, has high and variable extinction, and so it will be prudent to obtain IR photometry. This will allow us to estimate both the extinction and the intrinsic color of the star. Because our fields are quite crowded, we will need IR observations with high angular resolution, which can be obtained with adaptive optics (AO) systems

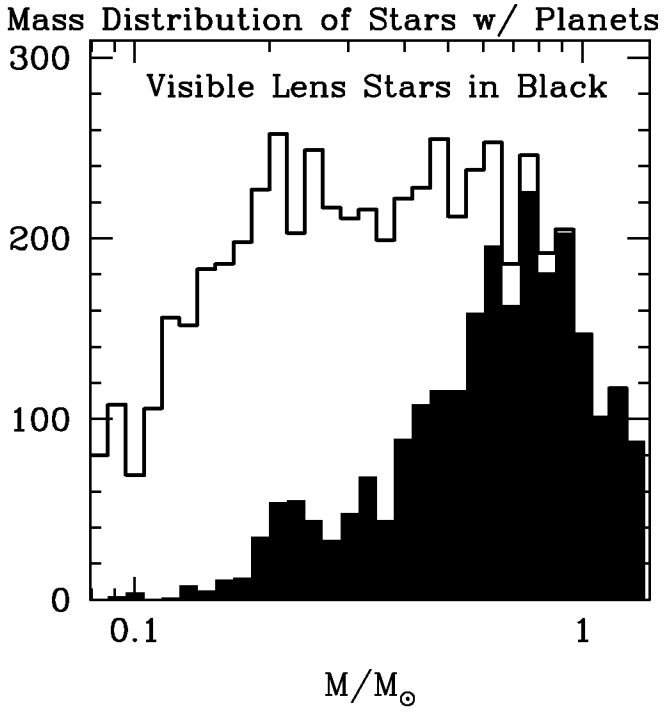

FIG. 11.—Simulated distribution of stellar masses shown for stars with detected terrestrial planets. Lens stars are considered visible when they are at least 10% of the brightness of the source star, if they are not blended with a brighter star (besides the source). One-third of the events have visible lens stars. [*See the electronic edition of the Journal for a color version of this figure.*]

on large telescopes such as the Very Large Telescope, Gemini, LBT, or Keck. The high stellar density of the microlensing survey fields implies that there are virtually guaranteed to be nearby guide stars to provide the phase reference needed for these AO systems. We would expect to obtain two sets of IR, AO observations: one during the event that would be scheduled as soon as the planetary signal is detected and the second set of observations taken well after the event is over. This pair of observations taken at different lens magnifications will allow us to unambiguously determine the color and brightness of the lens stars. We will require these data only for events with detected planetary signals, and so there should be no difficulty in obtaining the ground-based telescope time.

Another measurable parameter for the visible lens stars is the relative proper motion between the lens and the source, which is typically $\mu \approx 8$ mas yr^{-1} for a total motion of 32 mas over 4 yr. This is 15% of a CCD pixel for the sampling of the proposed *GEST* mission. Anderson & King (2000) argue that centroids can be measured to 0.2% of a pixel with a combination of a set of undersampled *HST* Wide Field Planetary Camera 2 frames that have been dithered to recover the resolution lost to undersampling. A space-based microlensing survey will provide more than 100 times more data than the most ambitious *HST* programs, which will allow numerous cross-checks to look for systematic errors in the centroid determinations. Thus, we expect that the centroids of the space-based stellar images can be determined at least as well as the centroids of the *HST* stars, so we expect to be able to measure the relative proper motion to an accuracy of a few percent. An independent measurement of the lens-source proper motion can be obtained for the events that exhibit planetary lens caustic crossing features. These comprise somewhat more than 50% of the events in which terrestrial planets are detected, and they allow the ratio of the angular radius of the star to the angular Einstein radius θ_E to be measured in the light-curve fit. Since the source star angular radius can be estimated from its brightness and color, an estimate of θ_E can be obtained. The ratio of the angular Einstein radius to the lens-source proper motion is $\theta_E/\mu = t_E$, the Einstein radius crossing time that can also be measured from the light curve, and so these measurements of μ and θ_E give equivalent information.

The measurement of μ or θ_E allows us to use the following relation for the lens star mass:

$$M_l = \frac{\theta_E^2 D_s c^2}{4G} \frac{x}{1-x}, \qquad (2)$$

where $x = D_l/D_s$, the ratio of the lens to source distances. This relation allows us to determine the difference between the source and lens distances when the lens is close to the source because it indicates that M_l, and hence the lens luminosity, depends sensitively on $1 - x = (D_s - D_l)/D_s$. This means that the Einstein radius R_E can be determined for all lens stars with a measurement of the lens star brightness and its relative proper motion μ or its color, which in turn implies that the planetary separation can be determined in physical units. The results of this determination are shown in Figure 12, which shows the measured separation for detected planets as a function of their orbital semimajor axis. For this plot, we have assumed that the change in the relative lens-source centroid can be measured to 2 mas, the

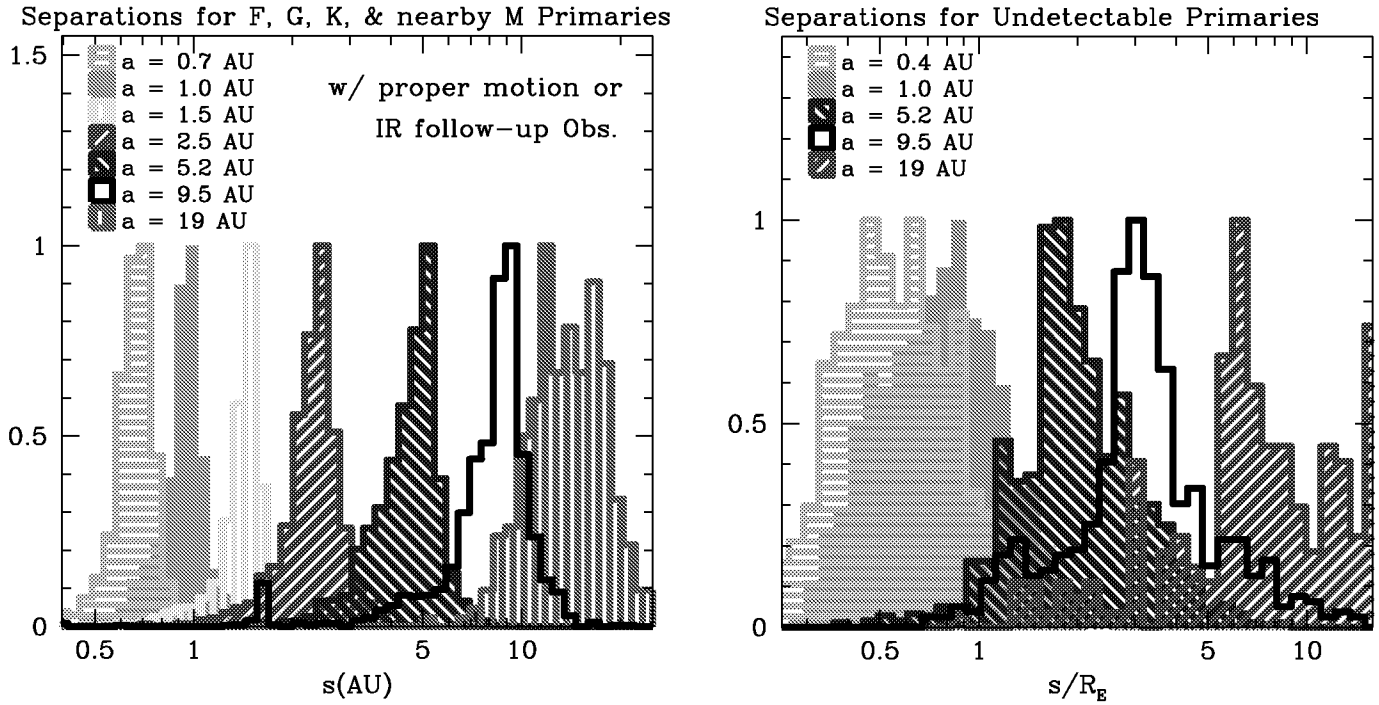

FIG. 12.—*Left*: Measured separation for planets with different orbital semimajor axes shown for the "visible" lens stars, for which the Einstein radius R_E can be determined. This allows the conversion of the measured separation s into physical units (AU). The following measurement accuracies are assumed: lens I_{lens}: 20%; $I - K_{lens}$: 10%; lens-source star centroids: 2 mas. The observed scatter in the measured separation relation is mostly due to the projection of the orbital plane on the sky. The distribution of measured star-planet separations is shown on the right for detected planets that orbit undetectable stars. The observed correlation between the planetary semimajor axis indicates that the measured separation can be used to estimate the semimajor axis with an accuracy of a factor of 2–3.

reddening-corrected I magnitude of the lens can be measured to an accuracy of 0.2 mag, and the reddening-corrected $I-K$ color can be measured to 0.1 mag. As Figure 12 indicates, the resulting estimate for planetary semimajor axis is accurate to about 20%. The uncertainty is dominated by the unmeasured the line of site component of the star planet-separation. When the lens star cannot be detected, the projected separation between the planet and its host star can only be measured in units of R_E. This can be used to estimate the planetary orbit semimajor axis by means of the expected correlation shown in the right-hand panel of Figure 12, which indicates that physical separation can be estimated with an accuracy of a factor of 2 or 3.

3.8. *Measurable Planetary Parameters*

The utility of planets that are detected by a space-based gravitational microlensing survey depends, of course, on the planetary properties that can be measured. For the ~33% of events with lens stars that are bright enough to be detected, the following parameters can be measured:

1. The mass of the planetary host (and lens) star is determined (with some redundancy) from the microlensing event timescale, the lens-source proper motion μ, and the source brightness and color.
2. The planetary mass M_{planet} is determined from the stellar mass and planetary mass fraction ϵ, which comes from the microlensing light-curve fit.
3. The distance to the planetary host star is determined from the same combination of parameters that gives the stellar mass.
4. The planet-star separation (in the plane of the sky) is always measured in units of the Einstein ring radius R_E. This can be converted to physical units when the lens star is detected.

For the remaining events with undetectable primary stars, the measurable parameters are the following:

5. The planetary mass fraction $\epsilon = M_{planet}/M_*$ is determined from the microlensing light curve.
6. The planet-star separation is measured in units of the Einstein ring radius R_E, and this can be converted to physical units with an accuracy of a factor of ~2.
7. The masses of the free-floating planets must generally be determined from the event timescale only. This can be done to an accuracy of a factor of 3 for each individual event.
8. Many of the ~1 $M_\oplus$ planets and virtually all of the ~0.1 $M_\oplus$ planets detected will have caustic crossing features that depend on the ratio of the source star radius to R_E. This will allow a mass estimate with an accuracy of a factor of 2 for planets orbiting a star or detected as isolated objects.

3.9. *Planet Detection via Transits*

While the focus of the space mission that we propose is to find low-mass planets via gravitational microlensing, the survey will also be sensitive to giant planets via transits of the ~10^8 Galactic bulge stars being monitored. Since giant planets like Jupiter have a radius that is about 10% of a solar radius, a transit of a Jupiter-like planet across the Sun will reduce the apparent brightness of the Sun by about 1%. The

TABLE 3
PLANETARY TRANSITS FROM *GEST*

Semimajor Axis (AU)	Period (yr)	Number of Detections	Transits per Planet	Transit Duration
0.04	~0.01	5000000	~200	1.6
0.4	~0.3	600000	~7	5
1.0	~1.3	160000	~2	8
2.0	~3.7	40000	1	11
5.2	~15	6000	1	18
9.5	~40	1300	1	24
19.5	~110	200	1	35

NOTE.—This table shows the number of expected transit planet detections for planets with a radius at least as large as that of Saturn for a 3 yr *GEST* mission assuming 8 months of observations per year. The planet detection numbers assume one planet per star.

proposed *GEST* telescope has the sensitivity to detect such a transit of a solar-type Galactic bulge star by a Saturn-size planet, and the following argument shows that such a mission can detect transits of Saturn-size planets orbiting fainter main-sequence stars as well (the planetary transits available from *GEST* are presented in Table 3). The luminosity and radius of a main-sequence star obey the following approximate relations: $L \propto M^{3.5}$ and $R \propto M$. Since the fractional photometric signal from a transiting planet (of a fixed radius) goes as R^{-2}, the signal-to-noise ratio for a transiting planet scales as $M^{-0.25}$, which is a very weak dependence slightly favoring lower mass stars.

Some of the $\sim 10^8$ target stars will have images that are blended with those of their near neighbor stars, and this can cause a substantial increase in the photon noise, which significantly reduces the sensitivity to planetary transits. This effect has been included in our calculations of the expected numbers of detectable planetary transits. The number of expected planetary transit detections for planets at different orbital distances is summarized in Table 1, which assumes a detection threshold of a 6.5 σ detection of a planet of Saturn's radius in 5 hr of exposures. This translates into a 9 σ detection of a Jupiter-sized planet. A crucial ingredient of our transit detection calculation is the inclusion of realistic stellar radii for the source stars because many of them have a radius that is substantially smaller than the Sun.

Planets with orbital periods longer than 4 yr can be detected via transits, but only one transit will be detected per planet. Such transits should have enough signal-to-noise ratio for a significant detection because the transit duration is $\lesssim 10$ hr, but the period of the planet can only be roughly estimated from the transit duration. Because of the huge number of stars that will be observed, planets out to ~20 AU are detectable even though there is only a probability of $\sim 2 \times 10^{-6}$ that such a planet would have its orbit aligned with the line of sight and have the right orbital phase to transit the source star during the period of observations. This sensitivity to distant planets via transits means that a space-based microlensing planet search mission will have a very substantial overlap in the planetary separations probed by the microlensing and transit techniques. At orbital distances of 0.4–20 AU, the proposed *GEST* mission will be sensitive to giant planets through both methods. This will allow cross-checks to help confirm the planetary interpretation of the transits. Since the transit signal indicates radius rather than mass, some of the transits could be caused by low-mass M dwarfs or brown dwarfs with similar radii but much larger masses than giant planets. Thus, some form of confirmation is desirable. For example, we might measure the radial velocities of some subsample of the candidate planets detected via transits using a moderate-resolution multiobject spectrograph. This would not allow us to distinguish between giant planets and low-mass brown dwarfs, but we should detect radial velocity variations for those stars that are transited by M dwarfs or high-mass brown dwarfs. This might allow a statistical correction for the nonplanetary transits.

With the combined sample of microlensing and transit detections of giant planets, a wide field-of-view space telescope will be able to probe the entire range of giant planet orbital radii: from 0, where the transit technique is very efficient, to ∞, where microlensing is the only viable technique. Thus, such a telescope promises a complete survey of giant planets with the combination of the two techniques.

3.10. *Additional Science with a Wide Field-of-View Space Telescope*

There are several other space-based microlensing planet search capabilities that we have not discussed in detail. Planets orbiting a single star of a binary system have been detected via radial velocities (Marcy & Butler 1996), and gravitational microlensing evidence has been presented for a planet orbiting a binary star system (Bennett et al. 1999), although this interpretation remains uncertain (Albrow et al. 2000) because of incomplete coverage of the microlensing light curve.

An additional capability that we have not discussed in this paper is the possibility of studying the abundance of planets in external galaxies, such as M31 (Covone et al. 2000). While most of the source stars in M31 will be either poorly resolved or unresolved by a telescope with angular resolution that is no better than that of *HST*, it is still possible to detect microlensing events with giant star sources if the microlensing magnification is not too small. Because an M31 planet search follows mostly giant source stars, it will not be very sensitive to terrestrial extrasolar planets, but it should be able to detect a large number of giant planets at a separation of 1–10 AU and measure their abundance as a function of position in the Galaxy.

Other possible science programs include a high-redshift supernova search and a deep, wide-field, high-resolution weak-lensing survey. (Both of these are goals of the proposed *SNAP* mission.) It would also be possible to carry out

a deep Kuiper belt object (KBO) search that should discover 100,000 new KBOs (Cook et al. 2000[9]). Many of these programs could be carried out during the 4 months per year when the Galactic bulge planet search field is too close to the Sun to be observed, and they might be selected as a part of a general observer program via a competitive review.

4. CONCLUSIONS

In this paper, we have presented the results of simulations of a space-based gravitational microlensing survey for terrestrial extrasolar planets, similar to the proposed *GEST* mission. We have determined the expected planet detection sensitivity as a function of the planetary mass fraction ϵ and the orbital semimajor axis, and we have shown how the sensitivity to Earth-like planets depends on the telescope parameters. We have found that such a mission will be sensitive to planets down to 1/10 of an Earth mass, or about 1000 times less than the masses of planets discovered with the radial velocity technique.

We have shown that a space-based microlensing planet search program should be able to directly detect the planetary host (and lens) stars for about one-third of the detectable planets. The observations of the host star when combined with the microlensing light curve will allow the determination of the planetary mass and separation as well as the stellar mass, type, and Galactocentric distance. The visible stars include virtually all of the "solar-type" lens stars, i.e., those of spectral type F, G, or K, which comprise about 25% of the total. For the remainder of the lens stars, which are mostly M dwarfs, it is generally possible to accurately determine the planetary mass fraction and to determine the projected planet-star separation to an accuracy of a factor of 2. For about one-third of the detected planets, the lens star should be directly detectable in the space-based survey data and with ground-based infrared observations (with adaptive optics). This allows an accurate determination of the mass and distance to the primary as well as the planetary separation in physical units.

The expected scientific output of a space-based microlensing planet search program is summarized as follows:

1. the average number of planets per star down to 0.1 $M_\oplus$ at separations of $\sim$0.7 AU–∞ for terrestrial planets and 0–∞ for giant planets;
2. the planetary mass function as a function of the planetary mass fraction, $f(M_{\rm planet}/M_*)$, and separation for all lens stars;
3. the planetary mass function as a function of stellar mass, Galactocentric distance, and the planet-star separation for G, K, and early M stars;
4. the abundance of giant planet pairs (a high abundance will indicate a large fraction of near circular orbits); and
5. the ratio of free-floating to bound planets as a function of planetary mass.

Finally, we would like to emphasize that the results that we have presented are based on very conservative assumptions. We have assumed a microlensing optical depth number that is 1.3 times smaller than the latest measurements indicate. If we assume that the optical depth measurement errors have a normal distribution, this is the 95% confidence level lower limit on the microlensing optical depth.

We have also been conservative in the selection of our planet selection criteria by demanding a 12.5 σ improvement ($\Delta\chi^2 \geq 160$) for a planetary microlensing fit compared to a single-lens fit. This ensures that we can make a reasonably accurate determination of the planetary parameters, but the event count could probably by increased by about 70% if the threshold was dropped to 9 σ. Furthermore, events with a peak magnification $A_{\rm max} > 200$ have not been included because they may be difficult to interpret. All told, if we dropped all of our conservative assumptions, we would have an event rate that is 2–3 times higher than we have reported (although the interpretation of some of these events might be difficult).

In summary, we have demonstrated that the space-based microlensing planet search mission can detect planets with masses down to that of Mars, which is 1/10 of an Earth mass and some 3 orders of magnitude better than current techniques. Space-based microlensing is unique among indirect terrestrial planet search programs in that low-mass planets are detected at high signal-to-noise ratios. Such a mission would be sensitive to terrestrial planets at orbital distances of $\gtrsim$ 0.7 AU via microlensing as well as giant planets at all orbital radii via both microlensing and transits. If each star has a 1 $M_\oplus$ planet orbiting at 1 AU, *GEST* would detect $\sim$100 of these. For about one-third of the detected planets, the host stars would be directly observable in the images. This will allow the determination of the stellar type, mass, and distance, and it will allow an accurate estimate of the planet-star separation in AU. The results we have presented indicate that a space-based microlensing planet search program could provide very useful statistics on the abundance of terrestrial and giant planets well in advance of the *TPF* mission, and this information would likely be quite useful in planning *TPF*.

We would like to thank John Mather for encouragement and advice during the early stages of this work, and we would also like to thank Domenick Tenerelli and his team at Lockheed Martin Space Systems for their efforts on behalf of the *GEST* Discovery proposal. Finally, we would like to thank the *GEST* co-investigators for their help. The co-investigators are I. Bond, E. Cheng, J. Connor, K. Cook, P. Garnavich, K. Griest, D. Jewitt, N. Kaiser, T. Lauer, J. Lunine, G. Luppino, D. Minniti, S. Peale, M. Shao, R. Stevenson, C. Stubbs, N. Woolf, and P. Yock. This work was supported, in part, by the NASA Origins grants NAG 5-4573 and NAG 5-9731.

[9] See footnote 3.

REFERENCES

Albrow, M. D., et al. 2000, ApJ, 534, 894
———. 2001, ApJ, 556, L113
Alcock, C., et al. 1997, ApJ, 479, 119 (erratum 500, 522 [1998])
———. 2000a, ApJ, 541, 270
———. 2000b, ApJ, 541, 734
———. 2000c, ApJ, 542, 281
Anderson, J., & King, I. R. 2000, PASP, 112, 1360
Beichman, C. 1998, Proc. SPIE, 3350, 719
Bennett, D. P., et al. 1997, in ASP Conf. Proc. 119, Planets beyond the Solar System and the Next Generation of Space Missions, ed. D. R. Soderblom (San Francisco: ASP), 95
———. 1999, Nature, 402, 57

Bennett, D. P., & Rhie, S. H. 1996, ApJ, 472, 660
———. 2000a, in ASP Conf. Ser. 219, Disks, Planetesimals and Planets Meeting, ed. F. Garzón, C. Eiroa, D. de Winter, & T. J. Mahoney (San Francisco: ASP), 198
———. 2000b, BAAS, 32, 32.10
Bertelli, G., Bressan, A., Chiosi, C., Fagotto, F., & Nasi, E. 1994, A&AS, 106, 275
Bissantz, N., Englmaier, P., Binney, J., & Gerhard, O. 1997, MNRAS, 289, 651
Bolatto, A. D., & Falco, E. E. 1994, ApJ, 436, 112
Butler, R. P., & Marcy, G. W. 1996, ApJ, 464, L153
Carr, M. H. 1996, Water on Mars (New York: Oxford Univ. Press)
Chyba, C. F., Whitmire, D. P., & Reynolds, R. 2000, in Protostars and Planets IV, ed. V. Mannings, A. P. Boss, & S. Russel (Tucson: Univ. Arizona Press), 1365
Cook, K. H., et al. 2000, BAAS, 32, 2101
Covone, G., de Ritis, R., Dominik, M., & Marino, A. A. 2000, A&A, 357, 816
Danner, R., & Unwin, S. 1999, *SIM*: Taking the Measure of the Universe (Washington, DC: NASA)
Deeg, H. J., et al. 2000, in IAU Symp. 202, Planetary Systems in the Universe: Observation, Formation and Evolution, ed. A. Penny (San Francisco: ASP), 108
Des Marais, D. J., et al. 2001, Jet Propulsion Laboratory publication, JPL 01-008 (Pasadena: JPL)
di Stefano, R., & Esin, A. A. 1995, ApJ, 448, L1
Dominik, M. 1999, A&A, 341, 943
Dressler, A., et al. 1996, *HST* and Beyond: Exploration and the Search for Origins: A Vision for Ultraviolet-Optical-Infrared Space Astronomy (Washington, DC: AURA)
Fridlund, C.,V. M. 2002, Planet. Space Sci., 50, 101
Gaudi, B. S. 1998, ApJ, 506, 533
Gaudi, B. S., & Gould, A. 1997, ApJ, 486, 85
Gaudi, B. S., Naber, R. M., & Sackett, P. D. 1998, ApJ, 502, L33
Gilliland, R. L., et al. 2000, ApJ, 545, L47
Gould, A., & Loeb, A. 1992, ApJ, 396, 104
Griest, K., & Safizadeh, N. 1998, ApJ, 500, 37
Han, C. 1997, ApJ, 490, 51
Han, C., & Gould, A. 1997, ApJ, 480, 196
Holtzman, J. A., Watson, A. M., Baum, W. A., Grillmair, C. J., Groth, E. J., Light, R. M., Lynds, R., & O'Neil, E. J., Jr. 1998, AJ, 115, 1946
Kasting, J. F. 1997, Origins Life Evol. Biosphere, 27, 291
Kasting, J. F., Whitmire, D. P., & Reynolds, R. T. 1993, Icarus, 101, 108
Koch, D. G., Borucki, W., Webster, L., Dunham, E., Jenkins, J., Marriott, J., & Reitsema, H. J. 1998, Proc. SPIE, 3356, 599
Kroupa, P. 2000, Astronomische Gesellschaft Abstract Ser. 16, T11
Lacy, C. H., Moffett, T. J., & Evans, D. S. 1976, ApJS, 30, 85
Lauer, T. R. 1999, PASP, 111, 1434
Levison, H. F., Lissauer, J. J., & Duncan, M. J. 1998, AJ, 116, 1998
Lunine, J. I. 1999, Earth: Evolution of a Habitable World (Cambridge: Cambridge Univ. Press)
———. 2001, Proc. Natl. Acad. Sci., 98, 809
Malhotra, R., Duncan, M. J., & Levison, H. F. 2000, in Protostars and Planets IV, ed. V. Mannings, A. P. Boss, & S. S. Russell (Tuscon: Univ. Arizona Press), 1231
Mao, S., & Paczyński, B. 1991, ApJ, 374, L37
Marcy, G. W., & Butler, R. P. 1996, ApJ, 464, L147
———. 2000, PASP, 112, 137
Marcy, G. W., Cochran, W., & Mayor, M. 2000, in Protostars and Planets IV, ed. V. Mannings, A. P. Boss, & S. S. Russell (Tuscon: Univ. Arizona Press), 1285
Mayor, M., & Queloz, D. 1995, Nature, 378, 355
McKee, C. F., & Taylor, J. H. 2000, Astronomy and Astrophysics in the New Millennium (Washington, DC: National Academy Press)
Peale, S. J. 1997, Icarus, 127, 269
———. 1998, ApJ, 509, 177
Perryman, M. A. C. 2000, Rep. Prog. Phys., 63, 1209
Popowski, P., et al. 2001, in ASP Conf. Proc. 239, Microlensing 2000: A New Era of Microlensing Astrophysics, ed. J. W. Menzies & P. D. Sackett (San Francisco: ASP), 244
Queloz, D., et al. 2000, A&A, 354, 99
Rhie, S. H., et al. 2000a, ApJ, 533, 378
———. 2000b, BAAS, 32, 32.06
Sackett, P. D. 1997, in Final Report of the ESO Working Group on the Detection of Extrasolar Planets, ESO Doc. SPG-VLTI-97/002, Appendix C
———. 1999, in Planets outside the Solar System: Theory and Observations, ed. J.-M. Mariotti & D. Alloin (Boston: Kluwer), 189
Schechter, P. L., Mateo, M., & Saha, A. 1993, PASP, 105, 1342
Schlegel, D. J., Finkbeiner, D. P., & Davis, M. 1998, ApJ, 500, 525
Schneider, J., et al. 1998, in ASP Conf. Series 148, ORIGINS, C. E. Woodward, J. M. Shull, & H. A. Thronson, Jr. (San Francisco: ASP), 298
Stanek, K. Z. 1999, ApJ, submitted (astro-ph/9802307)
Tytler, D. 1996, in A Road Map for the Exploration of Neighboring Planetary Systems, ed. C. A. Beichman (Washington, DC: NASA), chap. 7
Udalski, A., Szymanski, M., Kaluzny, J., Kubiak, M., Krzeminski, W., Mateo, M., Preston, G. W., & Paczyński, B. 1994, Acta Astron., 44, 165
Udalski, A., Zebrun, K. Szymanski, M., Kubiak, M., Pietrzynski, G. Soszynski, I., & Wozniak, P. 2000, Acta Astron., 50, 1
Wambsganss, T. R. 1997, MNRAS, 284, 172
Ward, P., & Brownlee, D. 2000, Rare Earth: Why Complex Life is Uncommon in the Universe (New York: Copernicus)
Ward, W. R. 1982, Icarus, 50, 444
Wozniak, P., & Paczyński, B. 1997, ApJ, 487, 55
Zoccali, C., Cassisi, S., Frogel, J. A., Gould, A., Ortolani, S., Renzini, A., Rich, R. M., & Stephens, A. W. 2000, ApJ, 530, 418